

EFFECTS OF THERMO-MECHANICAL
PROCESSING ON ALUMINUM-MAGNESIUM
ALLOYS CONTAINING HIGH WEIGHT
PERCENTAGE MAGNESIUM

Terry Lee Glover

NAVAL POSTGRADUATE SCHOOL

Monterey, California



THESIS

EFFECTS OF THERMO-MECHANICAL PROCESSING ON
ALUMINUM-MAGNESIUM ALLOYS CONTAINING
HIGH WEIGHT PERCENTAGE MAGNESIUM

by

Terry Lee Glover

December 1977

Thesis Advisor:

T.R. McNelley

Approved for public release; distribution unlimited.

T181127

SECURITY CLASSIFICATION OF THIS PAGE (When Data Entered)

REPORT DOCUMENTATION PAGE		READ INSTRUCTIONS BEFORE COMPLETING FORM
1. REPORT NUMBER	2. GOVT ACCESSION NO.	3. RECIPIENT'S CATALOG NUMBER
4. TITLE (and Subtitle) Effects of Thermo-Mechanical Processing on Aluminum-Magnesium Alloys Containing High Weight Percentage Magnesium		5. TYPE OF REPORT & PERIOD COVERED Master's Thesis; December 1977
7. AUTHOR(s) Terry Lee Glover		6. CONTRACT OR GRANT NUMBER(s)
9. PERFORMING ORGANIZATION NAME AND ADDRESS Naval Postgraduate School Monterey, California 93940		10. PROGRAM ELEMENT, PROJECT, TASK AREA & WORK UNIT NUMBERS
11. CONTROLLING OFFICE NAME AND ADDRESS Naval Postgraduate School Monterey, California 93940		12. REPORT DATE December 1977
		13. NUMBER OF PAGES 66
14. MONITORING AGENCY NAME & ADDRESS (if different from Controlling Office)		15. SECURITY CLASS. (of this report) Unclassified
		15a. DECLASSIFICATION/DOWNGRADING SCHEDULE
16. DISTRIBUTION STATEMENT (of this Report) Approved for public release; distribution unlimited.		
17. DISTRIBUTION STATEMENT (of the abstract entered in Block 20, if different from Report)		
18. SUPPLEMENTARY NOTES		
19. KEY WORDS (Continue on reverse side if necessary and identify by block number) Aluminum-Magnesium Alloys High Weight Percentage Magnesium		
20. ABSTRACT (Continue on reverse side if necessary and identify by block number) Cast ingots of three Al-Mg alloys, containing 7% Mg, 15% Mg, and 19% Mg, were obtained from Kaiser Aluminum and Chemical Corporation Center for Technology. Billets were machined from these castings and upset forged at .9% of either the solvus or eutectic temperature, as appropriate, to a true strain of 1.5. These alloys were then evaluated by compressive stress-strain testing at various temperatures and strain rates		

(20. ABSTRACT Continued)

to determine both the ambient and elevated temperature characteristics. Due to the inability to produce very fine second phase particles by upset forging, the 15% and 19% Mg alloys were high in strength but brittle at room temperature. However, refinement of the second phase particles during compression testing led to superplastic behavior at elevated temperature, with a strain rate sensitivity coefficient of .43 being achieved in the 19% Mg alloy. It was further observed that the addition of Mg increased strain rate sensitivity in these Al-Mg alloys at all temperatures, especially at elevated temperatures.

Approved for public release; distribution unlimited.

Effects of Thermo-Mechanical Processing on
Aluminum-Magnesium Alloys Containing
High Weight Percentage Magnesium

by

Terry Lee Glover
Lieutenant, United States Navy
B.S., United States Naval Academy, 1968

Submitted in partial fulfillment of the
requirements for the degree of

MASTER OF SCIENCE IN MECHANICAL ENGINEERING

from the

NAVAL POSTGRADUATE SCHOOL
December 1977

ABSTRACT

Cast ingots of three Al-Mg alloys, containing 7% Mg, 15% Mg, and 19% Mg, were obtained from Kaiser Aluminum and Chemical Corporation Center for Technology. Billets were machined from these castings and upset forged at .9% of either the solvus or eutectic temperature, as appropriate, to a true strain of 1.5. These alloys were then evaluated by compressive stress-strain testing at various temperatures and strain rates to determine both the ambient and elevated temperature characteristics. Due to the inability to produce very fine second phase particles by upset forging, the 15% and 19% Mg alloys were high in strength but brittle at room temperature. However, refinement of the second phase particles during compression testing led to superplastic behavior at elevated temperature, with a strain rate sensitivity coefficient of .43 being achieved in the 19% Mg alloy. It was further observed that the addition of Mg increased strain rate sensitivity in these Al-Mg alloys at all temperatures, especially at elevated temperatures.

TABLE OF CONTENTS

I.	INTRODUCTION -----	9
II.	EXPERIMENTAL PROCEDURES -----	13
	A. ALLOY ACQUISITION -----	13
	B. ORIGINAL PLAN -----	13
	C. REVISED PLAN -----	14
	D. UPSETTING -----	15
	1. Equipment -----	15
	2. Procedure -----	15
	E. COMPRESSION TESTING -----	16
	1. Equipment -----	16
	2. Procedure -----	16
	F. FOLLOW-ON EXPERIMENTS -----	19
III.	RESULTS -----	21
	A. AMBIENT TEMPERATURE -----	21
	B. ELEVATED TEMPERATURE -----	26
	C. MICROSTRUCTURAL ANALYSIS -----	28
IV.	CONCLUSIONS AND RECOMMENDATIONS -----	31
	A. CONCLUSIONS -----	31
	B. RECOMMENDATIONS -----	34
	LIST OF REFERENCES -----	64
	INITIAL DISTRIBUTION LIST -----	66

LIST OF TABLES

I.	Schedule of tests for compression testing of the 7% Mg alloy -----	17
II.	Schedule of tests for compression testing of the 15% and 19% Mg alloys -----	18
III.	Results of tensile testing of the 7% Mg alloy -	22
IV.	Results of ambient temperature compression tests on specimens previously tested at elevated temperature -----	23

LIST OF FIGURES

1.	As-cast ingots from Kaiser Aluminum and Chemical Corporation -----	36
2.	Specimens prior to upsetting, after upsetting, and prior to compression testing -----	37
3.	SEM photomicrograph of a 15% Mg alloy following upsetting -----	38
4.	SEM photomicrograph of 19% Mg alloy following upsetting -----	39
5.	Baldwin-Tate-Emery 60,000 lb. testing machine with heated platen arrangement, used for upset forging -----	40
6.	Instron Model TT-D floor model testing machine, used in compression stress-strain testing -----	41
7.	Marshall split furnace, used for temperature control during compression stress-strain testing -----	42
8.	As-cast 15% Mg alloy -----	43
9.	SEM photomicrograph of as-cast 19% Mg alloy -----	44
10.	19% Mg alloy following compression ₂ testing at 269 °C and $1.3 \times 10^{-3} / 1.3 \times 10^{-2} \text{ sec}^{-1}$ strain rate -----	45
11.	19% Mg alloy after compression testing at $T = 414 \text{ °C}$, $\dot{\epsilon} = 1.3 \times 10^{-3} / 1.3 \times 10^{-2} \text{ sec}^{-1}$ -----	46
12.	19% Mg alloy following compression testing at $T = 414 \text{ °C}$, $\dot{\epsilon} = 1.3 \times 10^{-4} / 1.3 \times 10^{-5} \text{ sec}^{-1}$ -----	47
13.	Compressive true stress vs. true strain for upset forged material at ambient temperature -----	48
14.	Log of true stress vs. log of true strain to determine n, work hardening exponent -----	49
15.	Compressive true stress vs. true strain for upset material at two strain rates and temperatures to 269 °C -----	50

16.	Compressive true stress vs. true strain curves for upset material at two strain rates and temperatures to 414 °C -----	51
17.	Log of true stress vs. log of true strain rate for the 7% Mg alloy -----	52
18.	Log of true stress vs. log of true strain rate for 15% Mg alloy -----	53
19.	Log of true stress vs. log of true strain rate for the 19% Mg alloy -----	54
20.	Strain rate sensitivity coefficient (m) vs. homologous temperature for 15% Mg and 19% Mg alloys -----	55
21.	Strain rate sensitivity vs. percentage Mg -----	56
22.	Flow stress vs. temperature for 7% Mg alloy at several strain rates -----	57
23.	Flow stress vs. temperature for 15% Mg alloy at several strain rates -----	58
24.	Flow stress vs. temperature for 19% Mg alloy at several strain rates -----	59
25.	SEM photomicrograph of an as-cast 7% Mg alloy --	60
26.	SEM photomicrograph of a 15% Mg specimen following compression testing -----	61
27.	Recast 19% Mg alloy with addition of 0.3% (by weight) Fe -----	62
28.	Recast 19% Mg alloy with addition of 0.3% Fe following upsetting at 300 °C -----	63

I. INTRODUCTION

The purpose of this research project was to continue the investigation toward development of thermo-mechanical processing treatments for aluminum magnesium alloys with high weight percentage magnesium. Following Bly, Sherby, and Young's success with hypereutectoid carbon steel [1], it was felt that a hypoeutectic Al-Mg alloy could be developed that would display a combination of ambient temperature strength and ductility equaling or exceeding that of conventional aluminum alloys, plus superplasticity at elevated temperatures. If this combination of properties could be realized, the material would have a higher strength-to-weight ratio, due to the large additions of Mg, than present aluminum alloys being used for ship and aircraft construction. In addition, such an alloy would be highly formable at elevated temperatures due to superplasticity. Superplasticity can lead to complex parts being formed in one operation [2] [3] [4].

In order to achieve any of the desired properties in such aluminum-magnesium alloys, a fine, homogeneous grain size and dispersion of the second phase must be developed by thermo-mechanical processing. The fine particles lead to high strength at ambient temperature by blocking dislocation movement [5] [6]. Fine particles also lead to greater ductility at room temperature through enhanced strain

hardening. A ductile matrix containing fine, hard particles is less apt to display brittleness since small particles will not crack as easily as large particles. Thus, crack initiation in the matrix will be inhibited, and ductility will be enhanced [7].

Fine microstructure is important to produce ambient temperature properties; and, in addition, such fine microstructure is also important with respect to superplastic properties at elevated temperatures. Superplasticity refers to extensive ductility, generally observed at elevated temperatures. For instance, under superplastic conditions, elongation to fracture may reach values as large as 2000% [2] in contrast to values of 50 to 100% which are more typical of conventional materials tested at the same temperature and strain rate.

According to Brick, Pense and Gordon [8], to exhibit superplasticity an alloy normally requires a fine grained microstructure, usually consisting of two plastic phases, with a grain size under 5 μm ; a stable structure at the superplastic deformation temperature, i.e., little or no grain growth; deformation at a temperature usually in the range 0.50 to 0.65 T_m (where T_m is the absolute melting temperature); and a controlled slow strain rate and high value of strain-rate sensitivity.

The basic mechanism for superplastic deformation according to Ashby and Verrall [9] is grain boundary sliding with diffusional accommodation. This mechanism is characterized

by non-uniform flow and exhibits the following general characteristics: (1) Grains do not exhibit the same shape change as the specimen; (2) grains switch nearest neighbors; (3) grains translate past each other by sliding at their boundaries; (4) by changing neighbors, the grains can remain unchanged in shape while the specimen exhibits a large change in shape. Fine grain and particle size enhances this boundary sliding with diffusional accommodation process [9], thus enhancing superplastic deformation of the material.

In Al-Mg alloys, the beta phase, which is an inter-metallic phase of composition Al_3Mg_2 , softens extensively upon heating [10]. Once a fine grain size in the aluminum matrix, and also a fine beta particle size, is realized, the interphase boundaries will migrate slowly, and thus a fine, stable grain size is maintained [3]. Thus, this system meets the requirements for superplasticity in that the mechanism as discussed by Ashby and Verrall becomes feasible.

In earlier research Ness [11] found that by hot rolling an as-cast 18% Mg alloy at temperatures ranging from 425°C down to approximately 300°C, a fine homogeneous microstructure was developed leading to compressive strengths in excess of 95 KSI at room temperature. Ness also observed the onset of superplasticity at elevated temperature, with a strain rate sensitivity coefficient (m) between .3 and .4 being achieved. Ness found the hot rolling process to be both

slow and difficult with surface cracks often originating at very low values of true strain.

In order to try and diminish the problems associated with Ness' thermo-mechanical process, it was decided to employ upset forging of the as-cast material prior to hot rolling. Upset forging is a less severe deformation process than rolling and thus would not be as apt to initiate cracking as would rolling. The initial upsetting would begin to break up the relatively coarse beta particles so that rolling could then be accomplished without the problem of cracking.

The forging process as implemented in this research was successful in breaking up the as-cast structure but did not produce the desired refinement in the beta particles. Nonetheless it was decided to investigate the deformation characteristics of these alloys in the forged condition as a function of temperature and strain rate and to consider as well the effect of magnesium content on deformation characteristics.

Concurrent with this research an investigation was conducted by Bingay [12] regarding the optimum thermo-mechanical process necessary to break up the as-cast microstructure more thoroughly than accomplished here.

II. EXPERIMENTAL PROCEDURES

A. ALLOY ACQUISITION

Three aluminum-magnesium alloys were chosen to conduct this investigation, representing a range of magnesium content. The three compositions selected were 11%, 15%, and 19% magnesium. The rationale for these alloys was that 15% Mg is the maximum solid solubility of magnesium in aluminum; it was decided to investigate the 15% alloy and, as well, compositions on either side. Several attempts were made to cast the alloys in the Naval Postgraduate School laboratories; however, due to lack of equipment and experience, castings were both small and porous, making further processing difficult. Kaiser Aluminum and Chemical Corporation was contracted to cast the 3 alloys as 2 1/4" X 4 1/2" X 12" ingots (See Figure 1.). Subsequent testing by atomic absorption suggested that the 11% alloy was actually 7% Mg by weight [12]. Moreover, the atomic absorption technique is relatively inaccurate for a magnesium content this high, and thus there is some uncertainty regarding the Mg content of this alloy.

B. ORIGINAL PLAN

The original plan of investigation was to fabricate 2" X 3/4" X 3/4" billets (See Figure 2a.) from the as-cast material. These billets would be upset forged (See Figure 2b.) at various temperatures and strain rates to determine the

best forging process. Subsequent hot rolling and extensive tensile testing and microstructural analyses were to follow. The objective was to determine the optimum thermo-mechanical process for producing the desired properties of increased strength to weight ratio and increased ductility at ambient temperature.

The upsetting procedure was accomplished on all alloys with no difficulty; however, hot rolling and subsequent tensile testing could be accomplished only on the 7% Mg alloy. Surface cracks during hot rolling on the 15% and 19% alloys prevented further processing and thus called for a revised plan of investigation. The inability to hot roll the 15% and 19% Mg alloys was later determined to be due to the coarse beta particles still present after upsetting (See Figures 3 and 4.).

C. REVISED PLAN

The revised plan of investigation was to eliminate the hot rolling and tensile testing. The three alloys would be upset forged, compression tested, and characterized. A separate investigation by Bingay [12] was then to be conducted to determine the processing conditions required to develop the desired microstructure for rolling and tensile evaluation of these materials.

D. UPSETTING

1. Equipment Description

All upset forging was conducted on a Baldwin-Tate-Emery testing machine with a 60,000 pound force capacity and variable cross head speeds. The heated platen arrangement shown in Figure 5 was used to control temperature during upsetting. A Hoskins electric furnace model FD202C was used to preheat all specimens prior to upsetting.

2. Procedures

In order to determine the best conditions for upsetting the three alloys, specimens were upset at different temperatures and crosshead speeds. These specimens were studied using the scanning electron microscope to determine which combination provided the finest microstructure. A crosshead speed of 1.66×10^{-3} inches per second and temperatures of 350°C for the 11% Mg alloy and 410°C for the 15% and 19% Mg alloys seemed to provide the finest microstructure.

Milled billets were prepared from the as-cast ingots in the Mechanical Engineering Machine Shop (See Figure 2a.). The billets were preheated to upsetting temperature for three minutes to reduce temperature gradients during upsetting. Following preheating the billets were upset using the aforementioned temperatures and crosshead speed to a true strain of 1.5. The billet was quenched in a fresh water quench to minimize grain and particle growth. The finished upset billet is shown in Figure 2b.

E. COMPRESSION TESTING

1. Equipment Description

All compression testing was conducted on an Instron Model TT-D floor model testing machine shown in Figure 6. This machine is capable of applying and recording loads up to 20,000 pounds with crosshead speeds from 3.3×10^{-5} inches per second to 3.3×10^{-1} inches per second.

The compression test assembly was designed to be compatible with the Instron testing machine. The assembly consists of a 1.0 inch diameter Haynes 188 punch and a 3.0 inch outside diameter Inconel cylinder with a 1.010 inch bore. The punch fits inside the test cylinder and slides on two machined lands inside the cylinder. Tungsten carbide platens are fitted in the punch and cylinder heads.

To conduct the compression tests at various temperatures, a Marshall split furnace, shown in Figure 7, capable of temperatures to 1200°C was utilized. Control of the furnace was provided by a Model #49 Omega proportioning control unit. Temperature variance was limited to $\pm 5^{\circ}\text{C}$ during the course of a compression test.

2. Procedures

Following the upsetting process the upset billets were milled to parallelepiped shaped test specimens .30 inch in length and .20 inch on a side as shown in Figure 2c. A total of 28 specimens of each alloy was tested in accordance with the schedules in Tables I and II. It should be noted

Table I - Schedule of tests for compression testing of the 7% Mg alloy. Strain rate changes from starting to finishing rates were accomplished at .15 true strain.

RUN	TEMP, °C	STARTING STRAIN RATE, SEC ⁻¹	FINISHING STRAIN RATE, SEC ⁻¹
1	25	1.3×10^{-4}	1.3×10^{-3}
2	..	3.23×10^{-4}	3.23×10^{-3}
3	..	6.45×10^{-4}	6.45×10^{-3}
4	..	1.3×10^{-3}	1.3×10^{-2}
5	53	1.3×10^{-4}	1.3×10^{-3}
6	..	3.23×10^{-4}	3.23×10^{-3}
7	..	6.45×10^{-4}	6.45×10^{-3}
8	..	1.3×10^{-3}	1.3×10^{-2}
9	151	1.3×10^{-4}	1.3×10^{-3}
10	..	3.23×10^{-4}	3.23×10^{-3}
11	..	6.45×10^{-4}	6.45×10^{-3}
12	..	1.3×10^{-3}	1.3×10^{-2}
13	217	1.3×10^{-4}	1.3×10^{-3}
14	..	3.23×10^{-4}	3.23×10^{-3}
15	..	6.45×10^{-4}	6.45×10^{-3}
16	..	1.3×10^{-3}	1.3×10^{-2}
17	282	1.3×10^{-4}	1.3×10^{-3}
18	..	3.23×10^{-4}	3.23×10^{-3}
19	..	6.45×10^{-4}	6.45×10^{-3}
20	..	1.3×10^{-3}	1.3×10^{-2}
21	315	1.3×10^{-4}	1.3×10^{-3}
22	..	3.23×10^{-4}	3.23×10^{-3}
23	..	6.45×10^{-4}	6.45×10^{-3}
24	..	1.3×10^{-3}	1.3×10^{-2}
25	347	1.3×10^{-4}	1.3×10^{-3}
26	..	3.23×10^{-4}	3.23×10^{-3}
27	..	6.45×10^{-4}	6.45×10^{-3}
28	..	1.3×10^{-3}	1.3×10^{-2}

Table II - Schedule of tests for compression testing of the 15% Mg and 19% Mg alloys, strain rate changes from starting to finishing rates were accomplished at .15 true strain.

RUN		TEMP °C	STARTING STRAIN RATE, SEC ⁻¹	FINISHING STRAIN RATE, SEC ⁻¹
15% Mg	19% Mg			
29	57	25	1.3×10^{-4}	1.3×10^{-3}
30	58	..	3.23×10^{-4}	3.23×10^{-3}
31	59	..	6.45×10^{-4}	6.45×10^{-3}
32	60	..	1.3×10^{-3}	1.3×10^{-2}
33	61	88	1.3×10^{-4}	1.3×10^{-3}
34	62	..	3.23×10^{-4}	3.23×10^{-3}
35	63	..	6.45×10^{-4}	6.45×10^{-3}
36	64	..	1.3×10^{-3}	1.3×10^{-2}
37	65	197	1.3×10^{-4}	1.3×10^{-3}
38	66	..	3.23×10^{-4}	3.23×10^{-3}
39	67	..	6.45×10^{-4}	6.45×10^{-3}
40	68	..	1.3×10^{-3}	1.3×10^{-2}
41	69	269	1.3×10^{-4}	1.3×10^{-3}
42	70	..	3.23×10^{-4}	3.23×10^{-3}
43	71	..	6.45×10^{-4}	6.45×10^{-3}
44	72	..	1.3×10^{-3}	1.3×10^{-2}
45	73	342	1.3×10^{-4}	1.3×10^{-3}
46	74	..	3.23×10^{-4}	3.23×10^{-3}
47	75	..	6.45×10^{-4}	6.45×10^{-3}
48	76	..	1.3×10^{-3}	1.3×10^{-2}
49	77	378	1.3×10^{-4}	1.3×10^{-3}
50	78	..	3.23×10^{-4}	3.23×10^{-3}
51	79	..	6.45×10^{-4}	6.45×10^{-3}
52	80	..	1.3×10^{-3}	1.3×10^{-2}
53	81	414	1.3×10^{-4}	1.3×10^{-3}
54	82	..	3.23×10^{-4}	3.23×10^{-3}
55	83	..	6.45×10^{-4}	6.45×10^{-3}
56	84	..	1.3×10^{-3}	1.3×10^{-2}

that each specimen was used for two different strain rates. The test apparatus was brought to desired temperature and allowed to stabilize before testing began. Each specimen was preheated in the compression chamber for 3 minutes prior to testing. In order to reduce the effects of triaxial stresses due to friction against the platens, Moly Dry Film Lubricant, a commercial product, was applied to the ends of each specimen.

A machine curve was generated to determine the intrinsic load-deflection characteristics of the Instron test machine. The results of this test indicated a spring constant of 232,558 pounds per inch for the machine and compression test apparatus.

F. FOLLOW ON EXPERIMENTS

After all analyses were completed on the preceding investigation, two more experiments were conducted. The first was to observe the effect of adding .3% Fe to the 19% alloy, and the second was to retest, at room temperature, specimens previously tested at elevated temperatures.

During the microstructural analysis of both the 15% Mg and 19% Mg alloys, the observation was made that the both as-cast and upset specimens had coarse beta particles (See Figures 3, 4, 8 and 9.) in contrast with Ness' findings [11]. A careful study of Ness' data indicated a small amount of Fe was present as well as small amounts of other elements. Therefore, the decision was made to investigate the effect of Fe on the as-cast material and the upsetting process.

A master 5% Fe alloy was cast using 99.99% pure Al and 20 mesh iron filings. Several billets of the as-cast 19% Mg alloy were then remelted and a small portion of the master alloy added to produce an 18% Mg alloy with .3% Fe. All casting was performed using furnaces in the Naval Post-graduate School Material Science Laboratory.

Following casting the billet was trimmed to 2 3/16" X 1" X 1" and upset forged at 300°C and a crosshead speed of 3×10^{-3} inches per second. These were considered to be the best parameters after studying the photomicrographs in Figures 10 through 12. Both as-cast and upset specimens were then microscopically observed.

During initial analysis it was observed that compression testing at elevated temperatures of previously forged material produced fine beta particles in the matrix between the coarse particles. This refinement is the major factor leading to increased strength at ambient temperature [5] [8]. Therefore, runs 72, 81, and 84 (See Figures 10, 11 and 12.) were retested at ambient temperature. The relative strength of the three specimens at a constant strain was compared to evaluate the effect of this additional, relatively fine beta.

III. RESULTS

It should be noted at the outset that there is uncertainty regarding the nominal 11% Mg alloy. During upsetting and compression testing it was believed to be 11% Mg. Temperatures were chosen for all processing that would keep the material in the two phase region (as an 11% Mg alloy). However some of the temperatures used were above the solvus line for 7% Mg. Therefore, some of the data for this 7% Mg alloy is perhaps in reference to a solid solution, single phase alloy.

A. AMBIENT TEMPERATURE MECHANICAL PROPERTIES

The results obtained from ambient temperature tensile testing of the 7% Mg alloy are presented in Table III. As the combination of upsetting speed and percentage reduction per pass increased, strength increased and ductility decreased. As was expected with this relatively low percentage Mg alloy, rolling was readily accomplished in run 13 with no prior upsetting.

The results obtained from ambient temperature compression testing of these alloys are presented in Figures 13 and 14. Also, Table IV presents ambient temperature compressive stress-strain results for samples retested after elevated temperature compressive deformation. Both the 15% Mg and 19% Mg alloys fractured at low strains. Though the fracture stress for both materials was about the same, the flow stress

Table III - Results of tensile testing of the 7% Mg alloy after upsetting and rolling. Upsetting temperature and rolling temperature was 330°C, true strain of upsetting was 1.7, percent reduction of rolling was 97%.

RUN	UPSET CROSSHEAD SPEED IN/SEC	ROLLING REDUCTION PER PASS %	UTS PSI	.2% YIELD	% ELONG
1	8.3×10^{-3}	≤ 1	52,300	37,100	14.5
2	1.6×10^{-3}	1	56,230	44,230	7.7
3	1.6×10^{-3}	1	54,956	47,772	8.95
4	1.6×10^{-3}	1	57,435	50,125	9.8
5	1.6×10^{-2}	2	62,638	59,417	5.7
6	1.6×10^{-2}	2	61,923	59,417	4.0
7	1.6×10^{-2}	2	63,421	61,209	3.4
8	1.6×10^{-2}	2	61,835	57,880	4.8
9	3.3×10^{-2}	5	60,945	57,772	4.8
10	3.3×10^{-2}	5	60,732	56,833	5.8
11	3.3×10^{-2}	5	61,555	57,272	5.4
12	3.3×10^{-2}	5	62,370	58,212	5.9
13	No Upsetting	Various	60,781	51,930	5.0

Table IV - Results of ambient temperature compression tests on specimens previously tested at elevated temperature. Stress is observed at a true strain of .04. All specimens are 19% Mg alloy, and strain rate is 1.3×10^{-2} inches per second.

PRIOR RUN #	PRIOR TEMP °C	PRIOR STRAIN RATE IN/SEC	STRESS
72	269	1.3×10^{-2}	81,000
84	414	1.3×10^{-2}	61,000
81	414	1.3×10^{-3}	44,000

at a given strain (prior to fracture) increased with increased magnesium. The opposite was true of ductility, in that as percentage magnesium increased, ductility decreased. Fracture occurred in the 15% and 19% Mg alloys when true strain equaled the work hardening exponent as determined in Figure 14. Figure 14 is based on the relationship between true stress and true strain as described by Dieter [7].

$$\sigma = K \epsilon_p^n \quad (1)$$

where σ is the true stress, ϵ_p is the plastic strain and K is a material constant. The exponent n is the strain hardening exponent.

Strain hardening, often called work hardening, is characterized by an increase in stress required to produce an increase in strain during plastic deformation. As can be seen from equation (1), strain hardening is greater as the strain hardening exponent (n) increases. At the beginning of plastic deformation, during a tensile test the cross-sectional area of a test specimen decreases, but the load-carrying capacity of the specimen increases due to strain hardening. Eventually, an elongation is reached where the incremental increase in load-carrying capacity due to strain hardening becomes less than the incremental decrease in load-carrying capacity due to decreasing load-bearing area, and the specimen cannot withstand further increase in load. The maximum load that the specimen can withstand is defined

as ultimate tensile strength, and the strain at this point is defined as true uniform strain [6] [7]. One can observe that the larger the strain hardening exponent n , the greater is the effect of strain hardening. This brings about a larger value of true uniform strain and thus a greater degree of ductility.

Dieter [7], based on the concept of tensile instability, predicts that true uniform strain equals the strain hardening exponent. It would be expected therefore that Ness' [11] material, with observed values of n up to 0.4, should be more ductile than these alloys which exhibit values of n less than 0.2. This, in fact, was the case and can be attributed to the large difference in beta particle size between these alloys and Ness' material.

The results of ambient temperature compression testing of samples previously tested at elevated temperatures are presented in Table IV. Although fracture occurred in each case at a low strain, there was a marked difference in the strength. The data indicates that the highest strength was achieved from the specimen previously tested at the lowest temperature and fastest strain rate. This result, to be further discussed, arises from further change in microstructure during elevated temperature deformation. Specifically, further precipitation and refinement of the beta inter-metallic phase occurs, leading to increased strength at ambient temperature.

B. ELEVATED TEMPERATURE MECHANICAL PROPERTIES

Figures 15 and 16 show the effects observed in the compression testing of the 15% Mg alloy. The 19% Mg alloy exhibited the same basic pattern. These materials exhibit a tendency toward strain softening at temperatures over 269°C, which is believed to result from microstructural refinement during compressive deformation at elevated temperature.

In an attempt to determine the degree of superplasticity exhibited by these materials at elevated temperature, the following equation was used:

$$\sigma = C\dot{\epsilon}^m \quad (2)$$

where C is a constant, m is the strain rate sensitivity coefficient, σ is the true stress and $\dot{\epsilon}$ is the strain rate. This equation has been proposed by several authors including Dieter [7], Alden [3], and Shelby and Burke [13] as describing the influence of strain rate on stress at elevated temperature. Figures 17 through 19 graphically illustrate the determination of m at various temperatures. The dependence of m on temperature is shown in Figure 20 for both 15% and 19% Mg alloys. The strain rate sensitivity coefficient (m) continually increases with temperature after the material has reached 0.5 of the eutectic temperature. This phenomenon — a smooth increase of m with temperature — was also observed by Alden [3] in other alloys which exhibit superplasticity.

For each temperature the strain rate sensitivity is larger for the 19% Mg alloy than for the 15% Mg alloy.

A plot of the maximum value of m obtained for each material versus weight percentage Mg in that material is shown in Figure 21. Strain rate sensitivity increases with percentage magnesium; the dashed line in Figure 21 is not intended to suggest a linear dependence per se, but rather a trend. Since this data is derived from tests at different temperatures in addition to different microstructures, the data indicates only an increase and not necessarily a linear relationship. Ayers [14] found that in working with low percentage Mg alloys ($\sim 4\%$ Mg), m also appeared to increase with percentage magnesium but not to values as large as observed here. It is surprising in some respects that these materials exhibit this trend toward superplastic behavior since the microstructure still contains large amounts of coarse beta. The beta particle size present after upsetting is $\sim 25\text{ }\mu\text{m}$ larger than usually observed in superplastic deformation.

The flow stress versus temperature behavior for these alloys is illustrated in Figures 22 through 24. At temperatures above 150°C to just below the eutectic point, there exists a consistent pattern between flow stress, temperature, and strain rate. Flow stress decreases with increasing temperature and increases with increasing strain rate. At lower temperatures there appears to be some degree of strain aging. This was observed by Ness [11] in an 18% Mg alloy

and is probably due to the Portevin-Le Chatelier effect [7]. The Portevin-Le Chatelier effect is evidenced when serrations occur in the stress-strain curve, and such serrations were observed at low temperatures (less than 100°C).

C. MICROSTRUCTURAL ANALYSIS

All specimens evaluated by microstructural analysis were prepared in exactly the same manner. Samples were abraded on successively finer sheets of emery paper to 000 and then polished by hand on rotating polishing cloth using slurries of alumina and water. Specimens were etched by immersion for one minute in 10% H_3PO_4 at a temperature of 50°C as recommended in reference [15]. All photomicrographs were taken on the S4-10 Stereoscan Scanning Electron Microscope (Cambridge Scientific Instruments Limited).

The as-cast alloys are shown in Figures 8, 9, and 25. Intermetallic beta particles (Al_3Mg_2) appear dark in the 7% alloy and are light areas in the 15% and 19% alloys. In both the 15% and 19% Mg alloys, the beta phase is chain-like and continuous throughout the material. It is evident, however, that the amount of beta increases with percentage magnesium. Upsetting the alloys to a true strain of 1.5 and at a temperature of 410°C tends to break up the chain-like particles of beta, but the particles are still quite large as shown in Figures 3 and 4.

Photomicrographs of 19% Mg specimens following compression testing are shown in Figures 10 through 12. The 15% Mg alloy

exhibited the same tendencies as the 19% Mg alloy (See Figure 26.). It is evident that the additional strain induced by the compression test (and the additional time at temperature) was instrumental in further breaking up and refining the beta particles. It is likely that some of the fine beta particles are formed by precipitation from the alpha solid solution matrix. Fine beta particles appeared within the alpha matrix plus fine beta particles at the alpha grain boundaries. Although these fine particles are now present, there is still coarse beta spread throughout the specimen. It should be noted that the coarse particles are finer than the original beta particles in the as-cast alloy.

The size of the fine particles in the alpha matrix and at grain boundaries is dependent on temperature and strain rate. A comparison of Figures 10 and 11 ($\dot{\epsilon}$ is constant for these data.) indicates that compression at a lower temperature develops finer beta particles. Bingay [12] found that temperatures as low as approximately 200°C may result in still finer particles being formed. A comparison of Figures 11 and 12 (temperature is constant) shows that a faster strain-rate also leads to finer particles. The strain rate in Figure 11 may not be the optimum but was the fastest employed in this investigation.

It was believed that the additions of small amounts of additional elements, such as Fe, might assist in refining the beta intermetallic phase. This was concluded by Bingay [12]

via chemical analysis of materials employed by Ness [11]. An analysis of the recast 19% Mg alloy with 0.3% Fe added is presented in Figures 27 and 28. The as-cast structure shows the beta particles greatly refined and much less continuous than the 19% Mg as-cast alloy. Following upsetting at 300°C, there was a much finer and more homogeneous dispersion of beta particles than was found in either the upset 19% alloy or the as-cast .3% Fe alloy. The fineness of the beta in the as-cast condition is likely due to the severe quench employed during re-casting. However, the homogeneity of the beta following upsetting is thought to be a function of the chemical composition. Again, however, coarse beta particles are present throughout the microstructure.

Important data has been presented on the influence of Mg on these high Mg alloys. However, the processing treatments employed have not resulted in an optimum microstructure for these alloys. The microstructures presented by Ness [11] were superior to those developed in this investigation and the ambient temperature properties obtained by Ness [11] were also better. It is believed that this is due to differences in processing treatments between this research and that of Ness [11]. The reasons for these differences will be discussed next, and current research is attempting to isolate those differences between Ness' [11] processing and that employed in this research to produce the desired microstructure.

IV. CONCLUSIONS AND RECOMMENDATIONS

A. CONCLUSIONS

The objective of this research, as stated previously, was to achieve an Al-Mg alloy which had high strength and ductility at ambient temperature and was also superplastic at elevated temperature. This objective was not fully realized; however, many discoveries were made which will lead to more complete understanding of the influence of thermo-mechanical processing on the microstructure of these alloys.

This investigation has re-emphasized the fact that beta particle size must be small in order to obtain a high degree of ductility at room temperature. Although compressive strengths in excess of 80 KSI were achieved for both 15% and 19% Mg alloys, ductility was very low. This was expected since the microstructure contained much coarse beta, and also the strain hardening coefficient (n) was relatively low for both alloys (See Figure 14.). As previously discussed, equation (1) predicts that when n is low, ductility will be low. Dieter [7] also predicts that n will increase as grain size decreases. The retesting of the specimens shown in Figures 10 through 12 revealed an increase in both strength and n with refinement of particle size in the microstructure.

The central problem encountered in regard to ambient temperature ductility was the failure to break up and refine

the coarse beta resulting from casting. It was initially believed that working the material at high temperatures under isothermal conditions would be successful. In Ness' [11] research, materials were rolled starting at a high temperature ($T = 400^{\circ}\text{C}$); necessarily, the billet temperature would drop, since the billet was in contact with the much colder rollers of the rolling mill. In contrast, the processing employed entailed forging on preheated platens to maintain nearly constant billet temperature during forging. It was initially believed that this difference in procedure was insignificant and that the materials being hot and concurrently worked were what led to the very fine microstructures developed by Ness [11], i.e., that the coarse beta developed in casting was being broken up. It is now evident that this was not the case. It appears likely that the fine microstructure produced by Ness was in large part a result of working as billet temperature decreased and that most of the microstructural refinement in his alloys was a result of working as beta precipitated from solid solution on cooling. In addition, the hot working of the material at a lower finishing temperature would inhibit grain growth. In fact, several sources support the theory of finishing hot working at a temperature just above recrystallization temperature in order to obtain fine grains [7] [16]. The results obtained by the forging method with heated platens were very encouraging in that the process was quickly and rapidly accomplished, with no signs of cracking, even with the coarse as-cast material.

Recent experiments, conducted after the bulk of this work was complete, indicate that a much finer microstructure can be obtained by initially solution treating the material at 435°C and subsequently forging at 300°C. It is believed that forging at the lower temperature causes refinement of the beta concurrent with its precipitation from the super-saturated solid solution.

It appears that increasing additions of Mg increases the strain rate sensitivity coefficient (m) and thus would be expected to produce a greater degree of superplasticity (See Figure 21.). However, with the addition of Mg, ductility at room temperature was decreased, at least for the relatively coarse microstructure present. In applications this trade-off of formability at elevated temperature versus ambient temperature ductility must be addressed.

The addition of Fe to the alloy seemed to have some refining effect on the as-cast microstructure and to play a part in the breaking up of beta during upsetting. However, the degree of refinement attainable under more optimal conditions remains to be determined. More research must be done on the effect of additional elements before a definite conclusion can be reached.

At high temperatures the strain rate sensitivity of the 15% Mg matched or exceeded that found by Ness [11] for an 18% Mg alloy. Realizing the possibility that both compositions are nominal and could be equal, it is a fact that Ness achieved a much finer and homogeneous microstructure. This

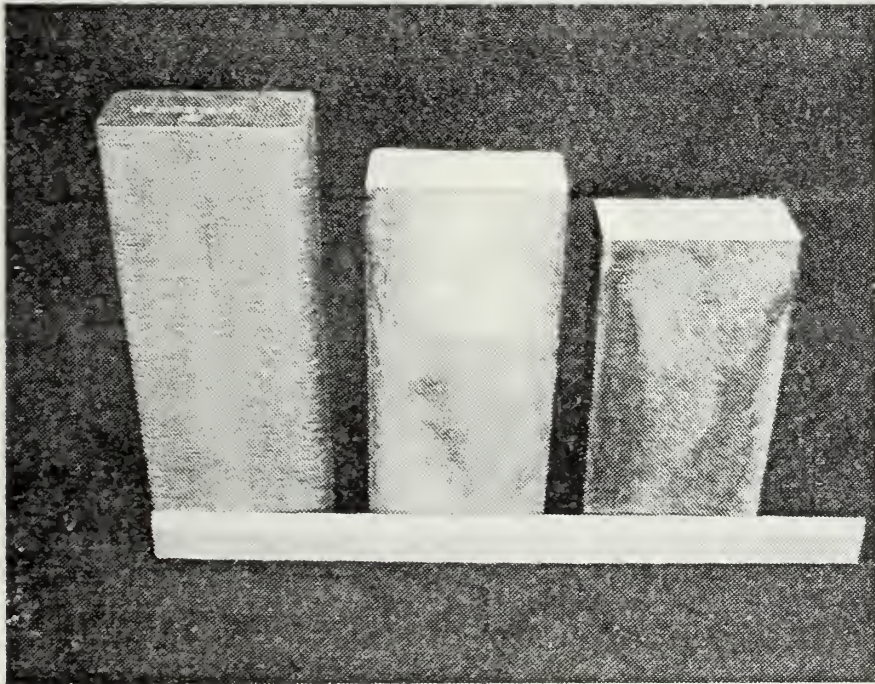
should lead to a higher value of M and thus to a greater degree of superplasticity. One can only surmise that once superplasticity is achieved, further refinement of the particles has little or no effect on superplasticity. In fact, it is somewhat surprising that the strain rate sensitivity coefficient was as large as it was (0.43). The as-forged microstructure is very coarse (approximately 25 μm) in particle size, and most research into this phenomenon would suggest a smaller value of the strain rate sensitivity coefficient for these materials. On the other hand, precipitation of fine particles does occur during elevated temperature testing, and it is likely that this refinement of the forged microstructure allows the rate sensitivity coefficient to reach the values attained. Note again, however, the marked difference in room temperature characteristics.

This research plus the work of Ness [11] and Bingay [12] have provided a base of information heretofore not known about Al-Mg alloys with large amounts of magnesium. This knowledge indicates that a thermo-mechanical process can be developed that will lead to an alloy characterized by a high strength-to-weight ratio so badly needed in modern Naval applications.

B. RECOMMENDATIONS

It is recommended that this research be continued with emphasis on three areas. First, investigate the upset forging

process while controlling temperature so as to finish at a temperature just above recrystallization. Second, investigate the difference between working of the coarse beta present in the cast alloys and working of beta as it precipitates from solid solution. Third, research must be accomplished in the area of chemical composition; there is a distinct possibility that a small amount of some element could be instrumental in grain refinement during mechanical working.

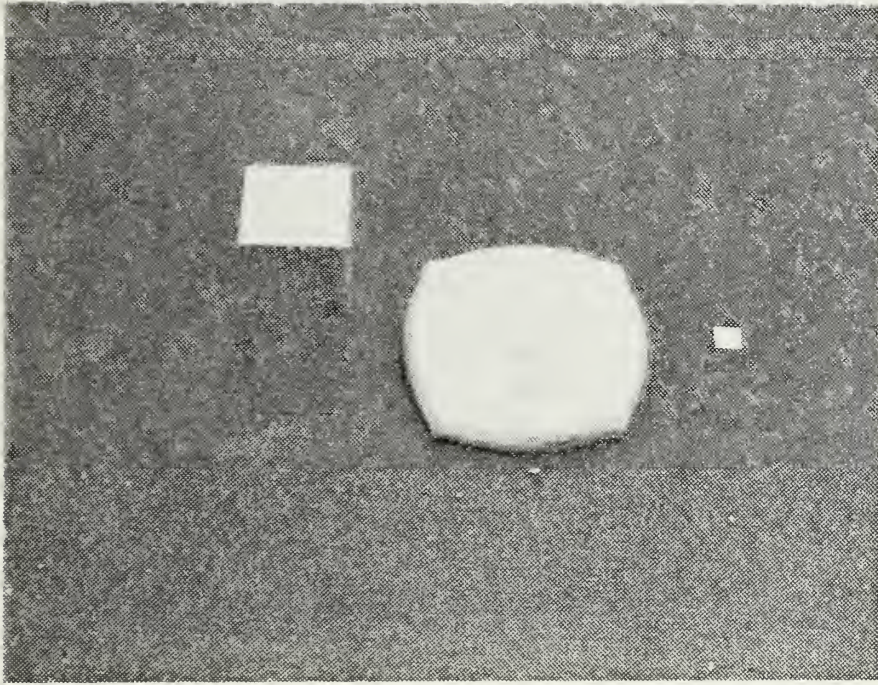


a

b

c

Figure 1. As-cast ingots from Kaiser Aluminum and Chemical Corporation. These ingots are nominally 2.25 inches by 4.5 inches in cross section, and were initially approximately 12 inches in length.
a) 7% Mg, b) 15% Mg, c) 19% Mg.



a

b

c

Figure 2. Specimens prior to upsetting, after upsetting, and prior to compression testing.

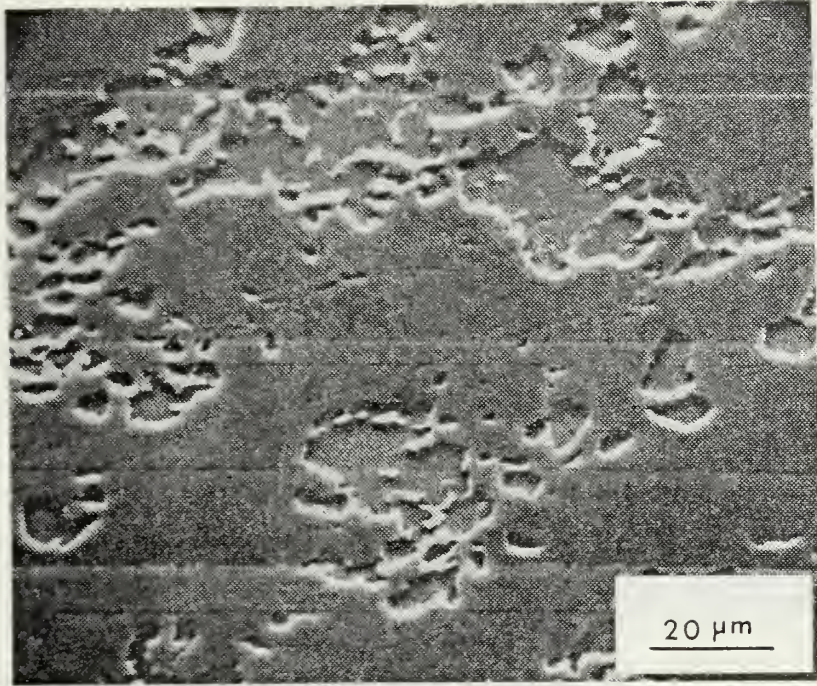


Figure 3. SEM photomicrograph of a 15% Mg alloy following upsetting. Upsetting conditions were: temperature = 410°C, crosshead speed = .1 inch per minute, total strain = 1.5. The chain-like appearance of the as-cast beta has been broken up, but particles are still large, 780X.

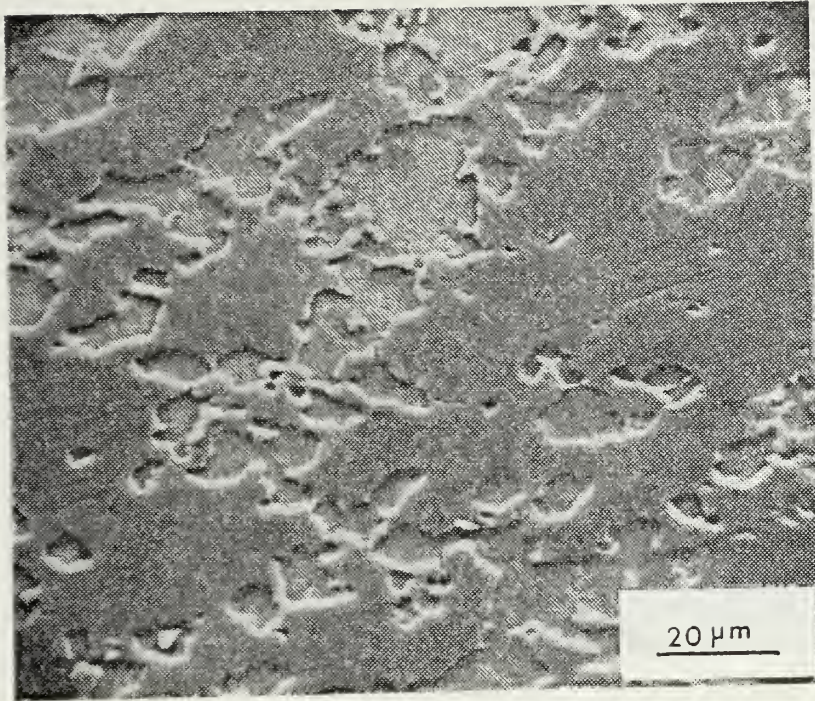


Figure 4. SEM photomicrograph of 19% Mg alloy following upsetting. Upsetting conditions were: $T = 410^{\circ}\text{C}$, crosshead speed = .1 inch per minute, total strain = 1.5. Continuity of beta is broken, however particles are still large, creating brittleness, 770X.

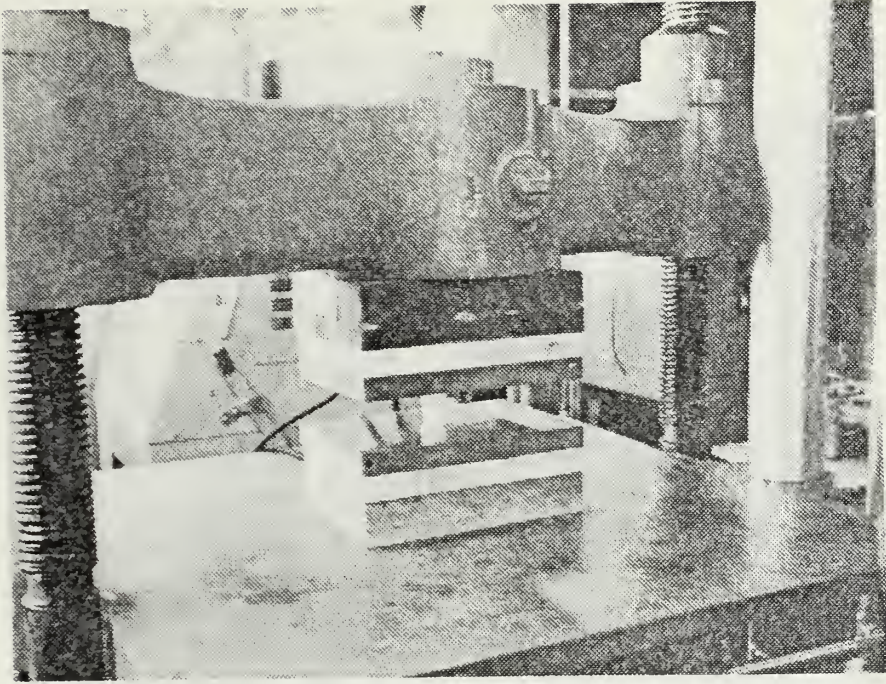


Figure 5. Baldwin-Tate-Emery 60,000 lb. testing machine with heated platen arrangement, used for upset forging.

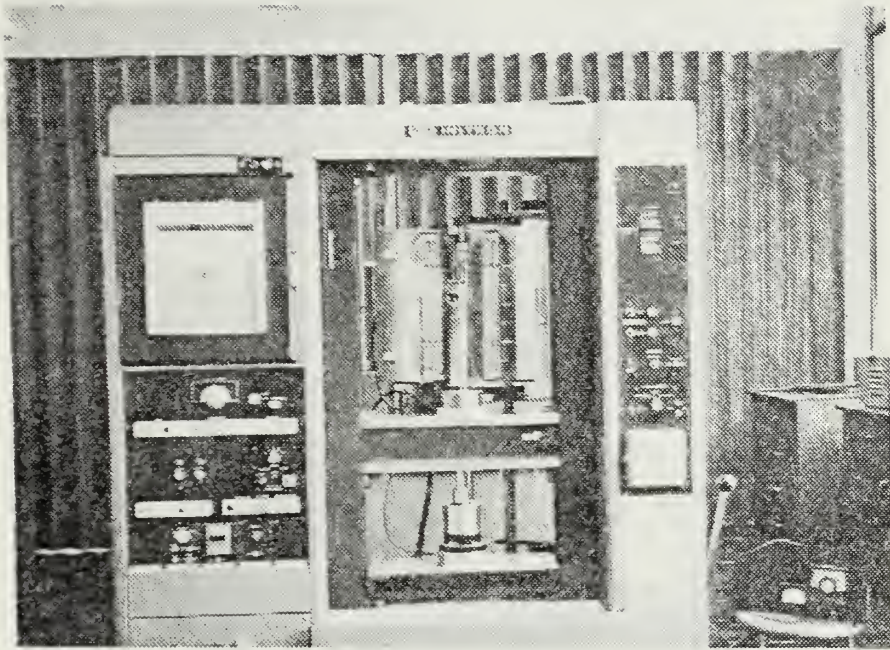


Figure 6. Inston Model TT-D floor model testing machine, used in compression stress-strain testing.

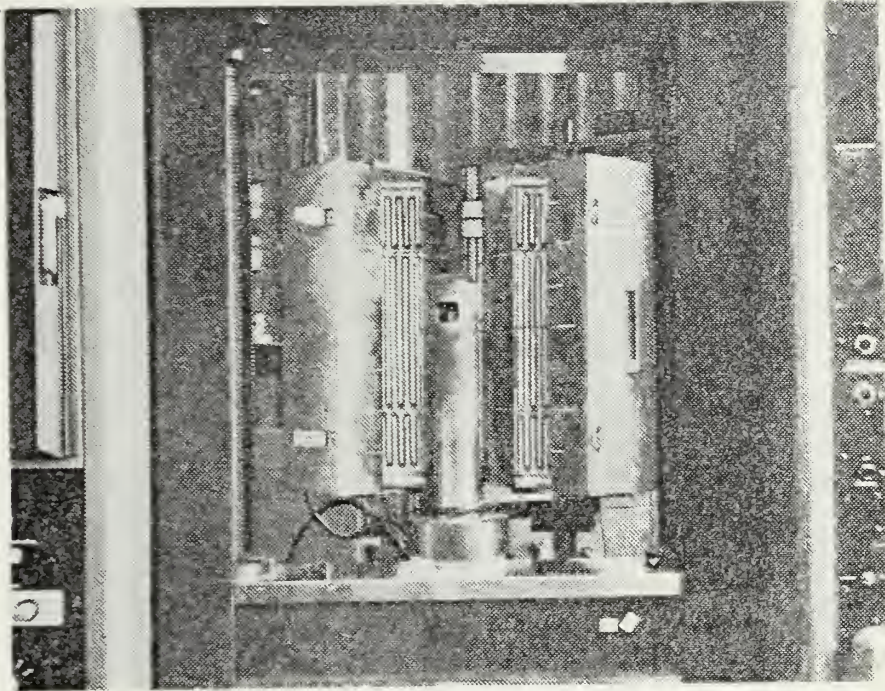


Figure 7. Marshall split furnace, used for temperature control during compression stress-strain testing.

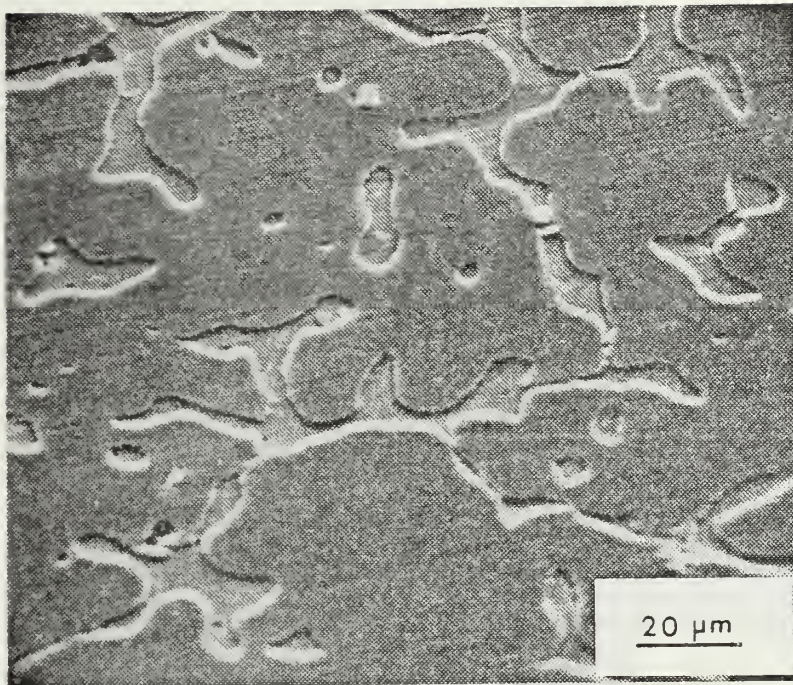


Figure 8. As-cast 15% Mg alloy. The light area is intermetallic beta phase and is continuous throughout the material. Some smaller beta particles are present but most beta is in the chain-like structure, 650X.

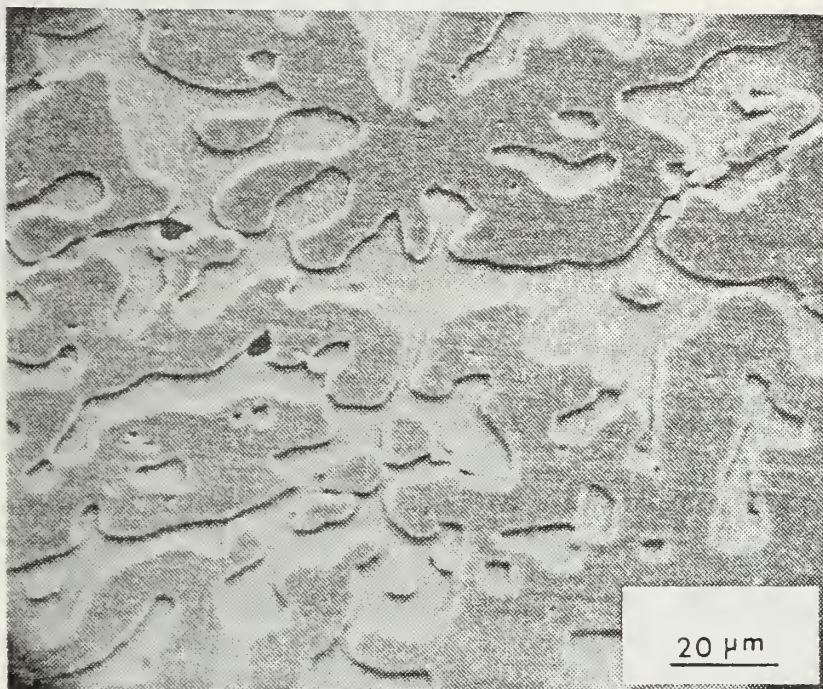
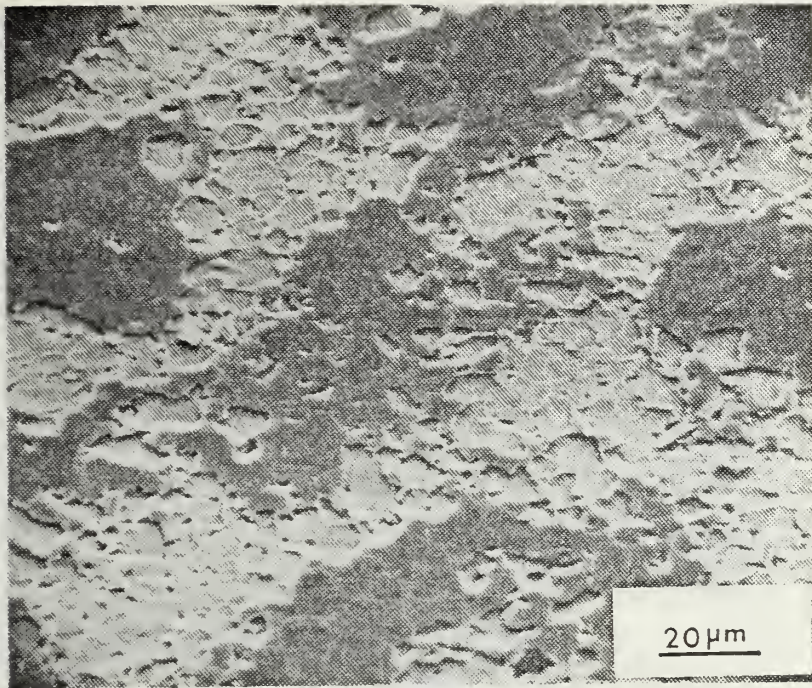
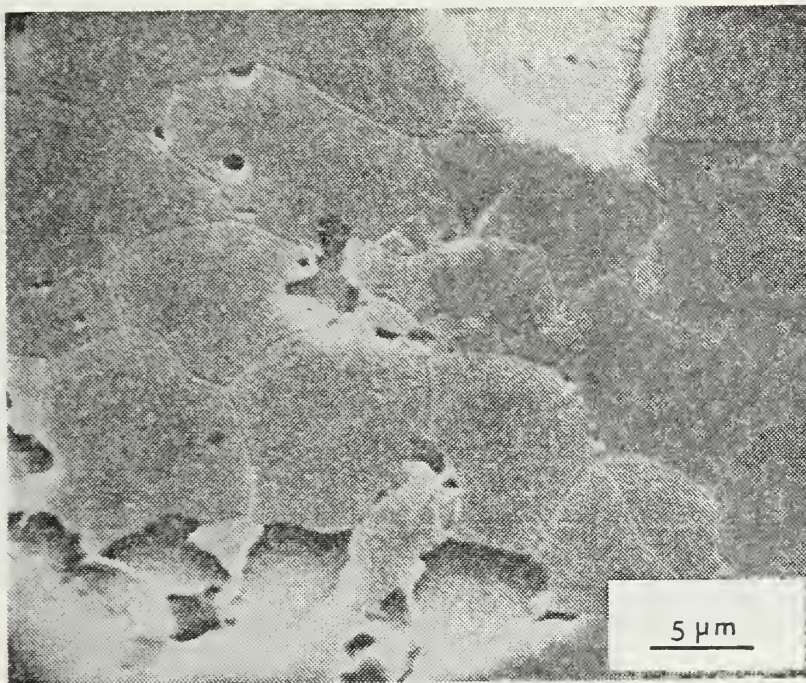


Figure 9. SEM photomicrograph of as-cast 19% Mg alloy. Beta phase is chain-like and continuous throughout creating a brittle as-cast material, 680X.

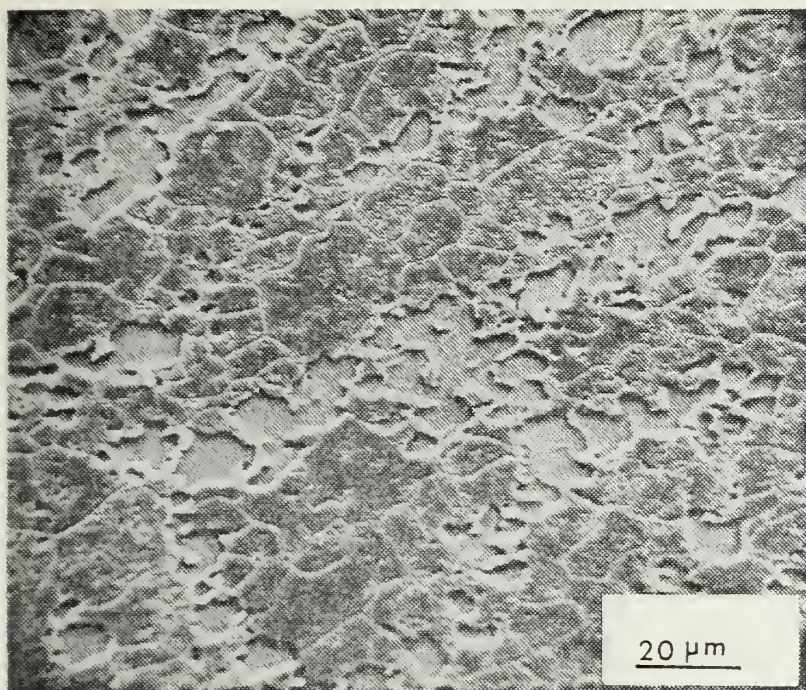


650X

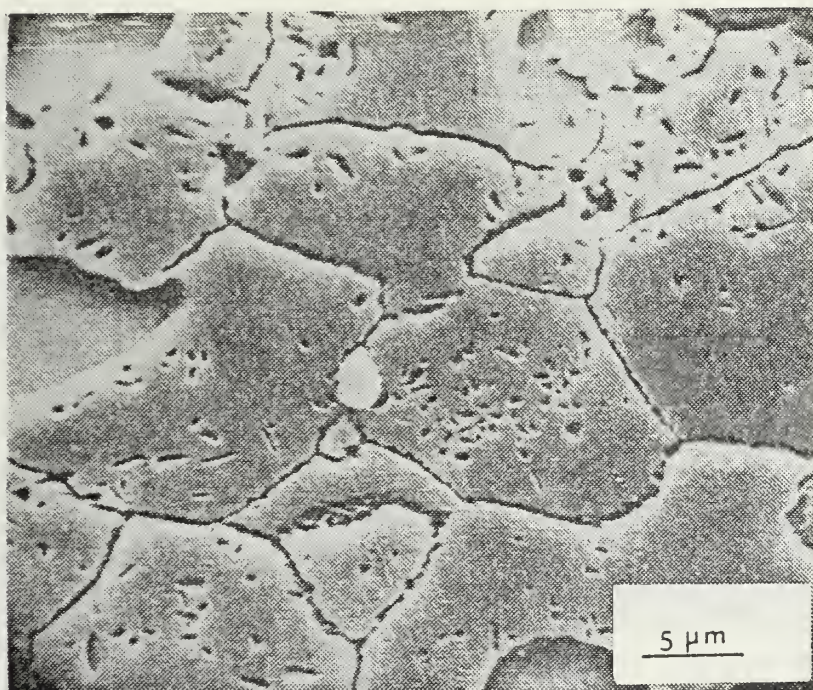


2600X

Figure 10. 19% Mg alloy following compression testing at 269°C and $1.3 \times 10^{-3} / 1.3 \times 10^{-2} \text{ sec}^{-1}$ strain rate. Refinement of beta has begun with beta now present at alpha grain boundaries. Even though refinement has begun large particles are still evident; there also appears to be some very fine beta within the alpha grain.

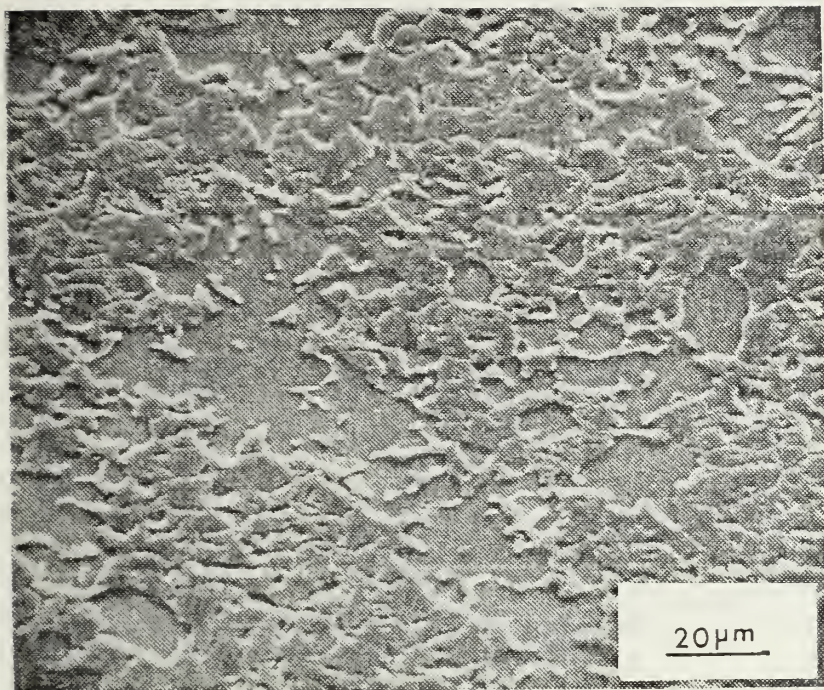


670X

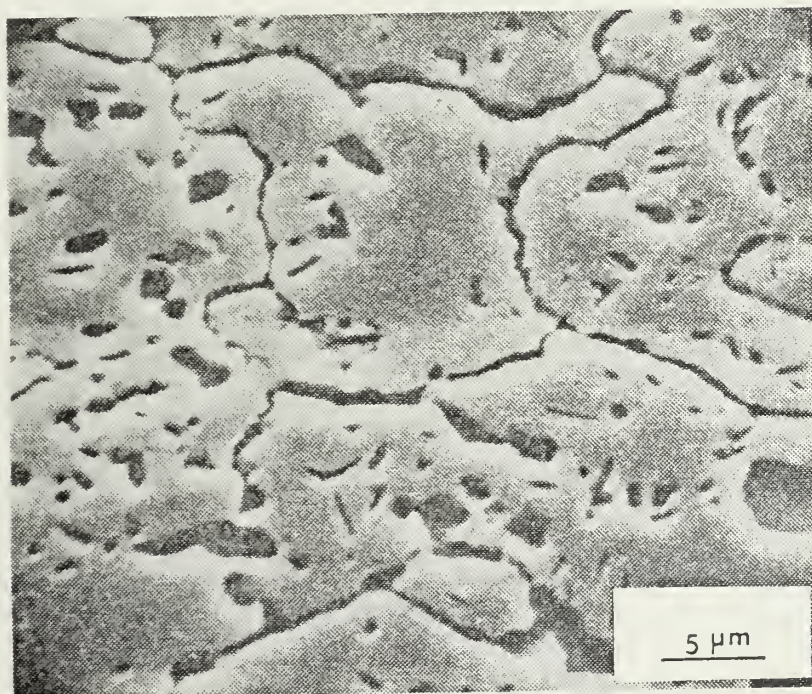


2600X

Figure 11. 19% Mg alloy after compression testing at $T = 414^{\circ}\text{C}$, $\dot{\epsilon} = 1.3 \times 10^{-3} / 1.3 \times 10^{-2} \text{ sec}^{-1}$. Fine particles of beta are present within the alpha matrix plus fine particles at grain boundaries. Beta particles forming within the alpha are coarser at this higher temperature.



670X



2700X

Figure 12. 19% Mg alloy following compression testing at $T = 414^{\circ}\text{C}$, $\dot{\epsilon} = 1.3 \times 10^{-4} / 1.3 \times 10^{-3} \text{ sec}^{-1}$. Beta particles are in alpha matrix and at grain boundaries but are much larger than those obtained at same temperature and faster strain rate (see Figure 11).

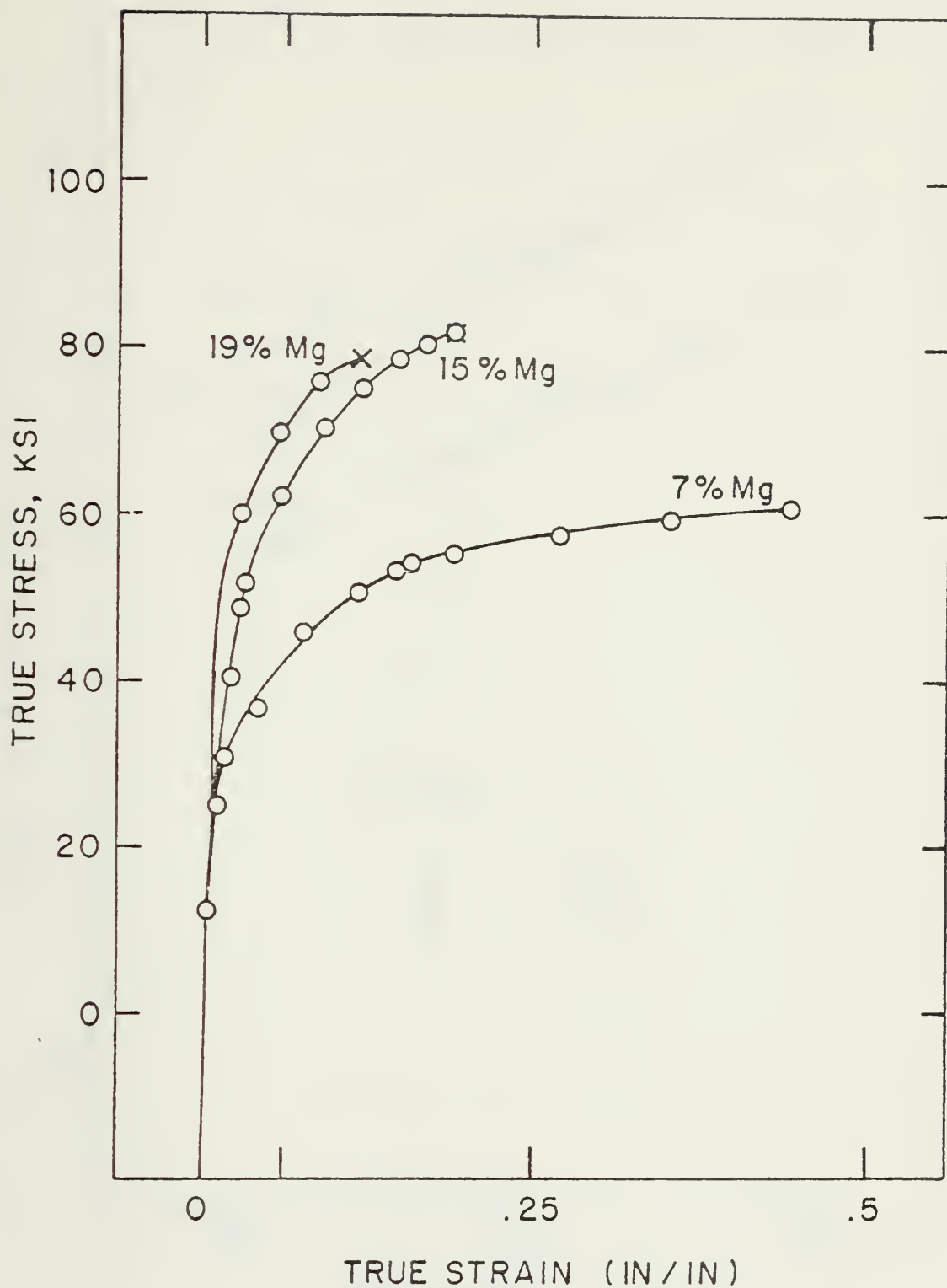


Figure 13. Compressive true stress vs. true strain for upset forged material at ambient temperature. Both 15% and 19% fractured at low strains due to presence of large particles of the beta phase.

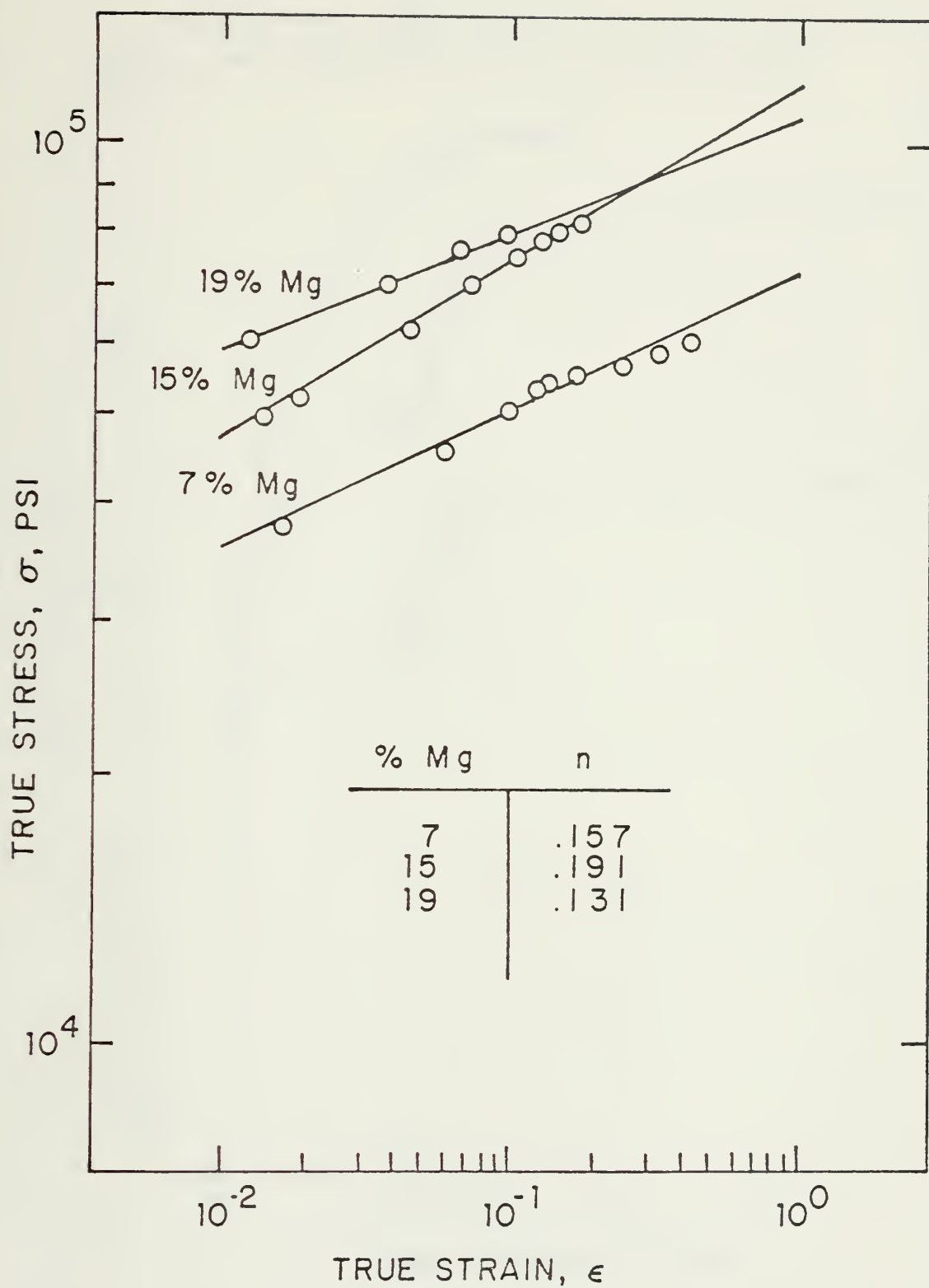


Figure 14. Log of true stress vs. log of true strain to determine n , work hardening exponent. Test temperature was room temperature.

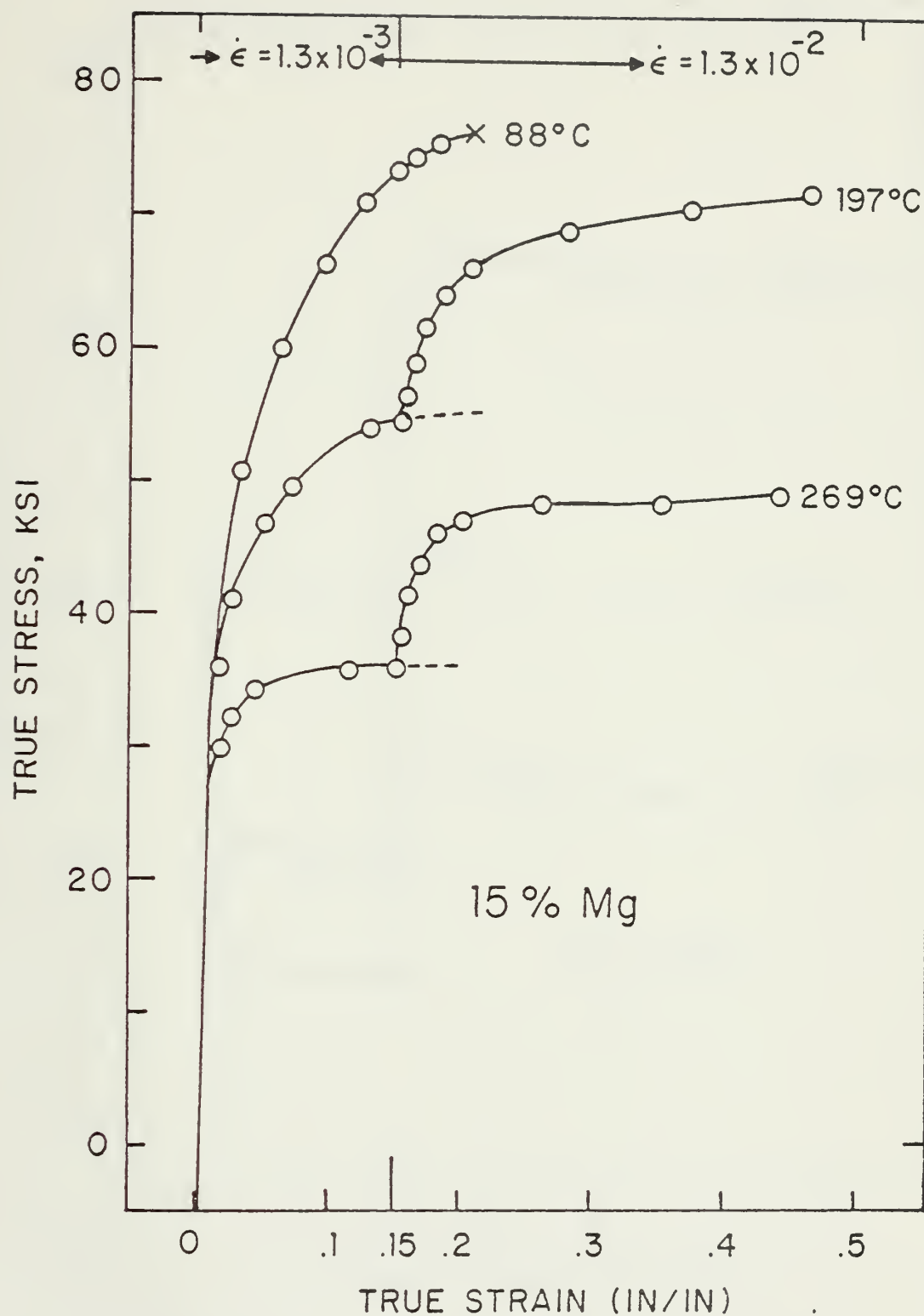


Figure 15. Compressive true stress vs. true strain for upset material at two strain rates and temperatures to 269°C. Strain rates were increased at .15 true compressive strain.

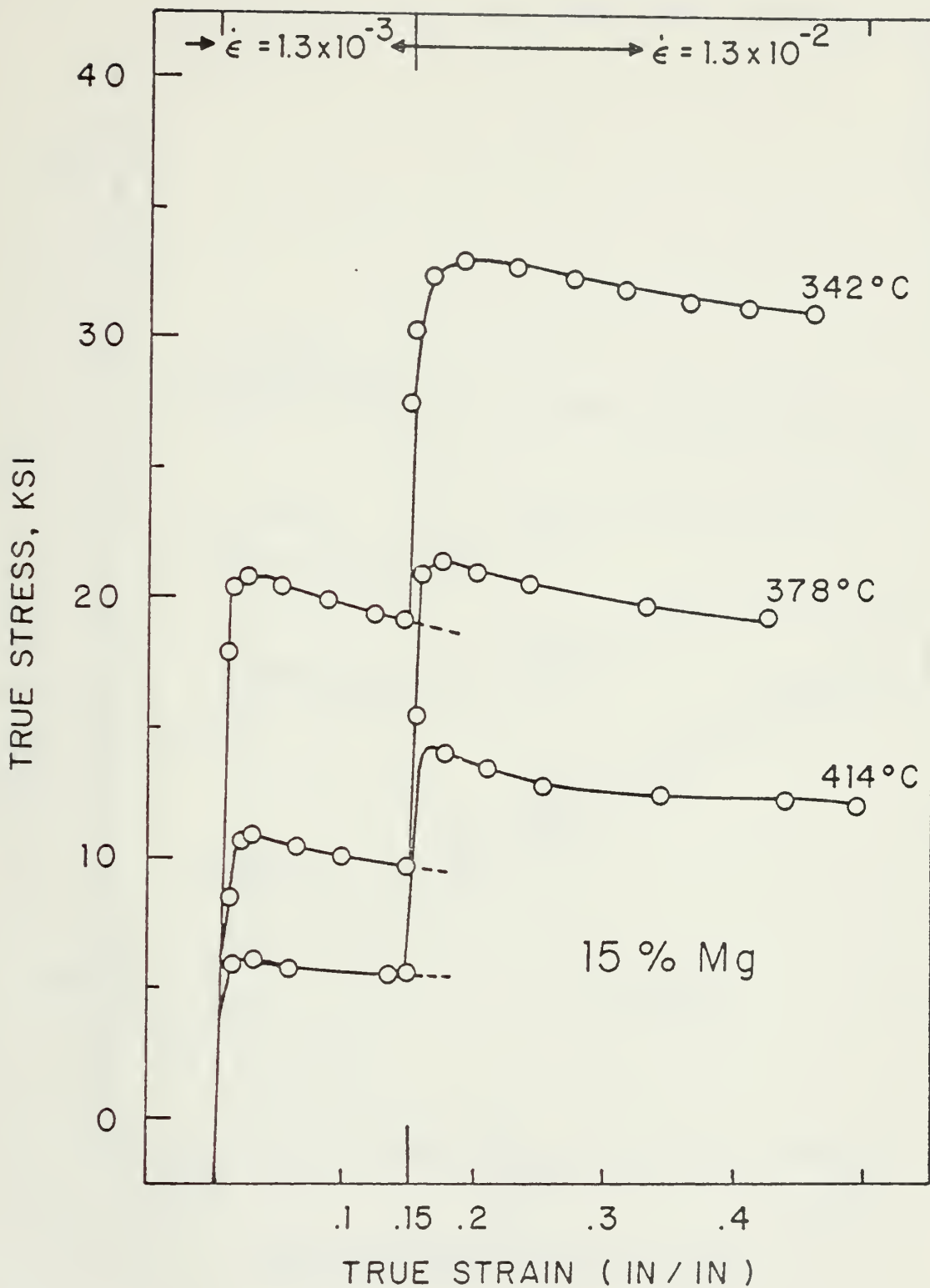


Figure 16. Compressive true stress vs. true strain curves for upset material at two strain rates and temperatures to 414°C. Strain rates were increased at .15 true compressive strain.

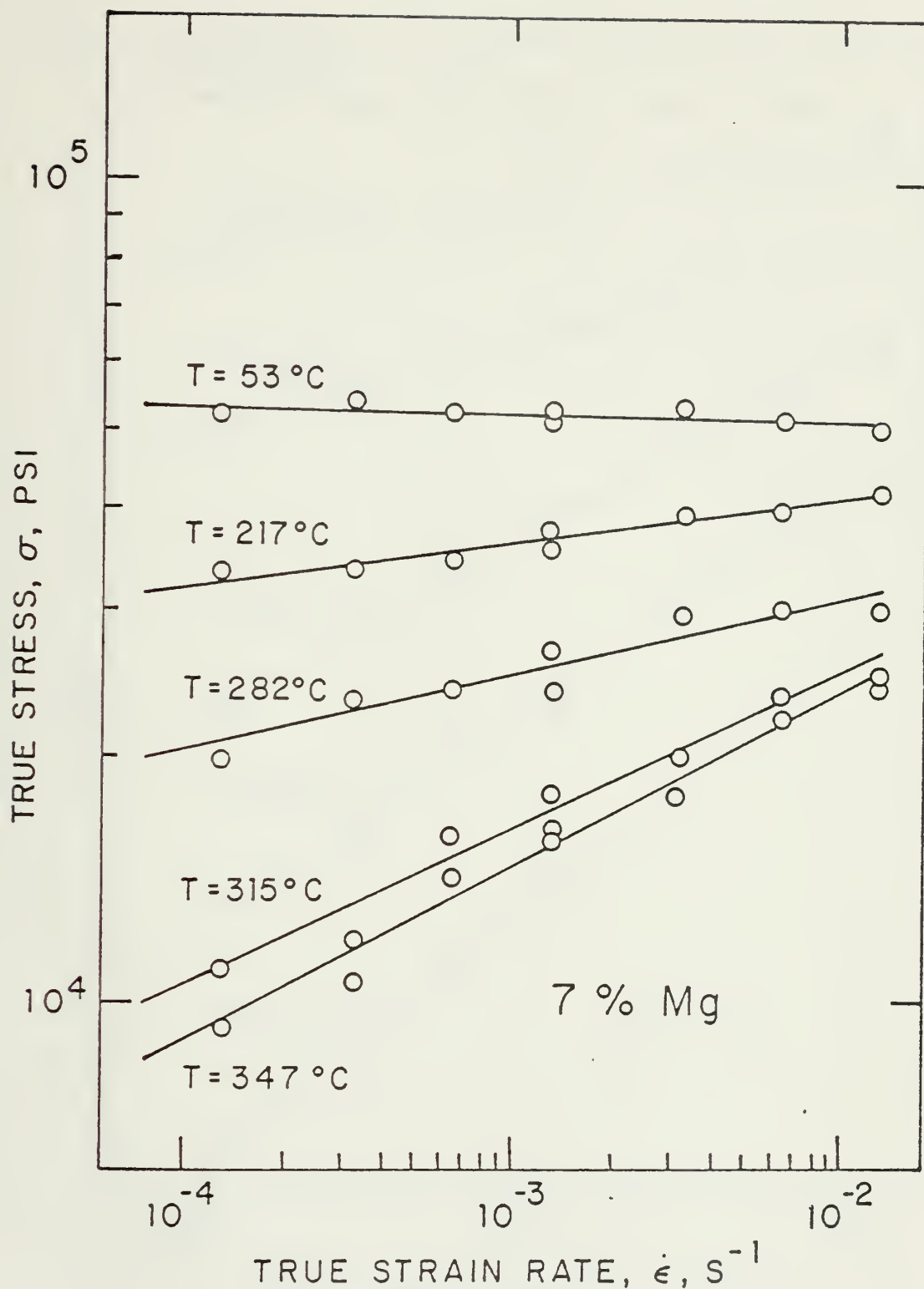


Figure 17. Log of true stress vs. log of true strain rate for the 7% Mg alloy. The slope of each line equals the strain rate sensitivity coefficient (m), which increases with temperature.

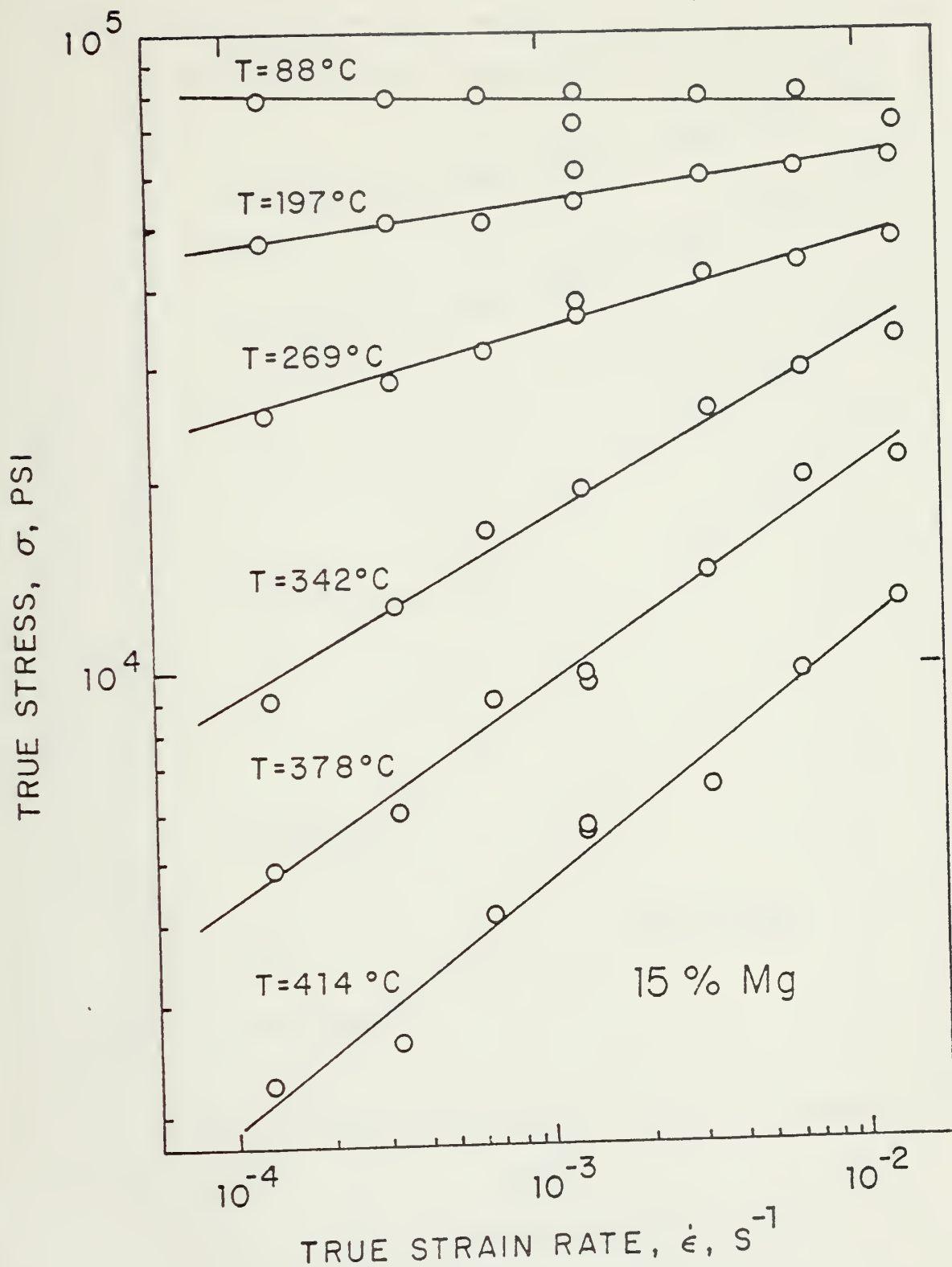


Figure 18. Log of true stress vs. log of true strain rate for 15% Mg alloy. The slope of each line equals the strain rate sensitivity coefficient (m), which increases with temperature. The maximum value of M is 0.389 for this material.

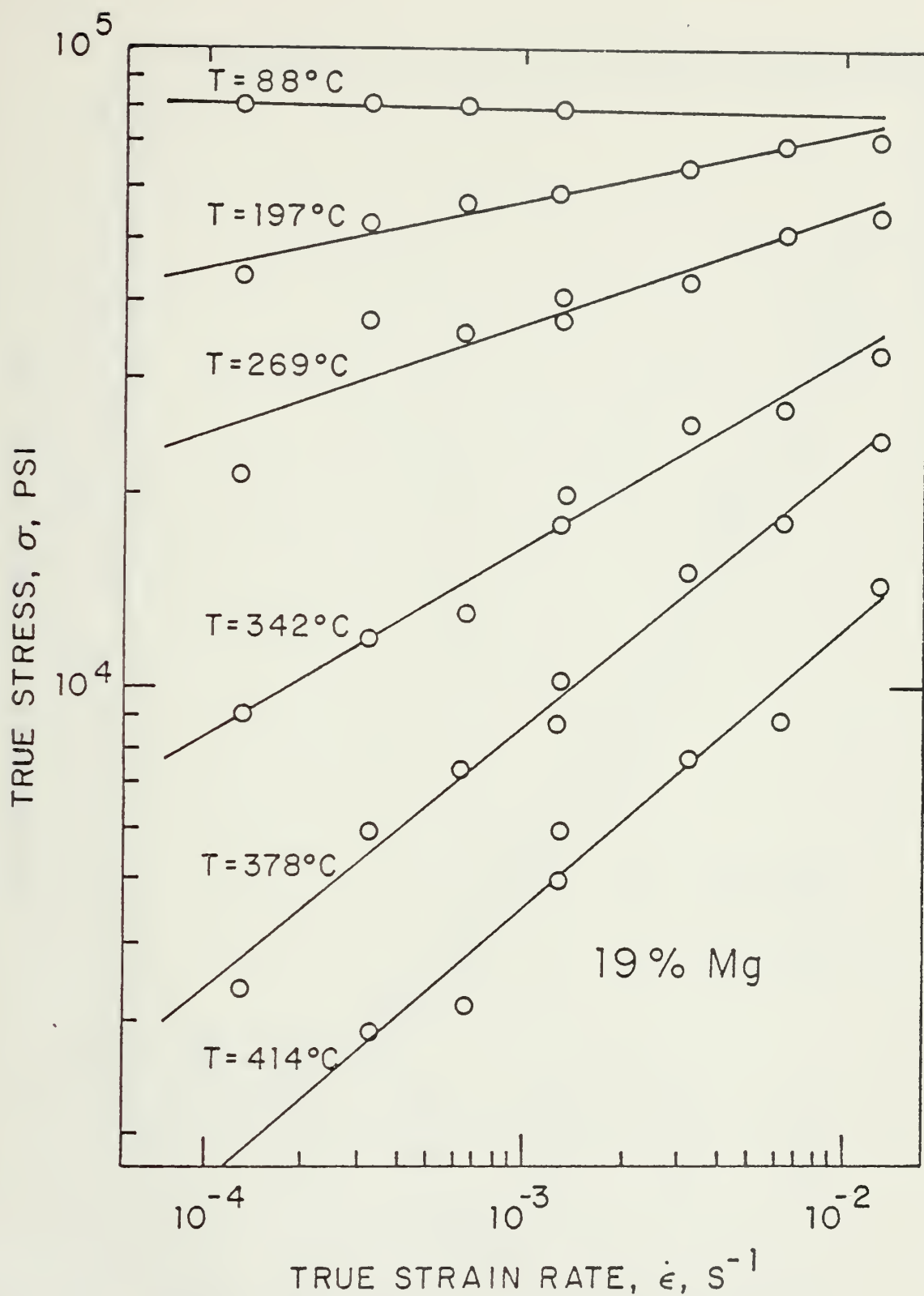


Figure 19. Log of true stress vs. log of true strain rate for the 19% Mg alloy. The slope of each line equals the strain rate sensitivity coefficient (m) which increases with temperature. The maximum value of M is 0.4345 for this material.

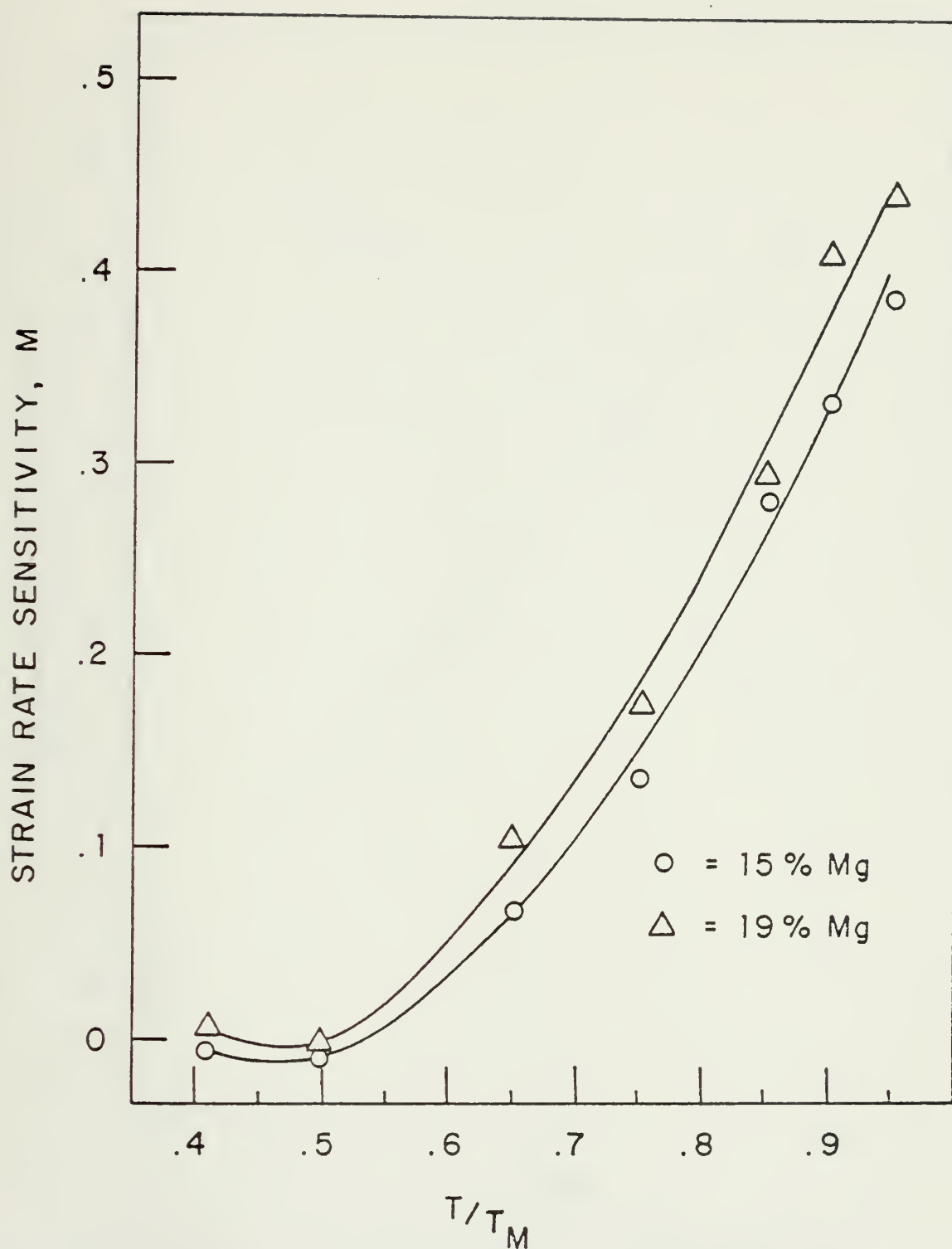


Figure 20. Strain rate sensitivity coefficient (m) vs. homologous temperature for 15% Mg and 19% Mg alloys. M increases with temperature and is always larger for the 19% alloy. Here T_m is the eutectic temperature (451°C).

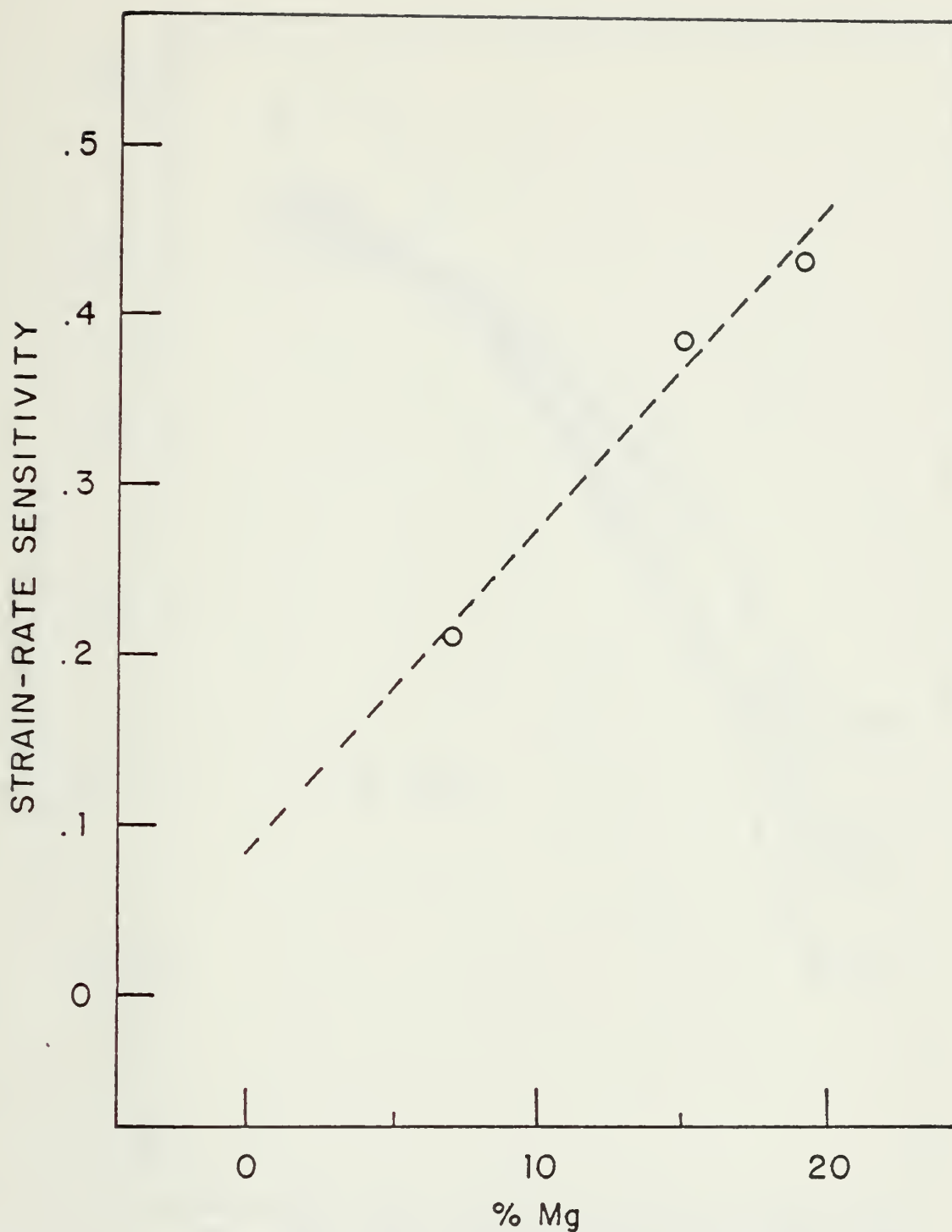


Figure 21. Strain rate sensitivity vs. percentage Mg. Each point is the maximum M obtained during testing each alloy. Dotted line indicates an increase in M as % Mg is increased due likely to increased beta in these alloys as percentage Mg increases.

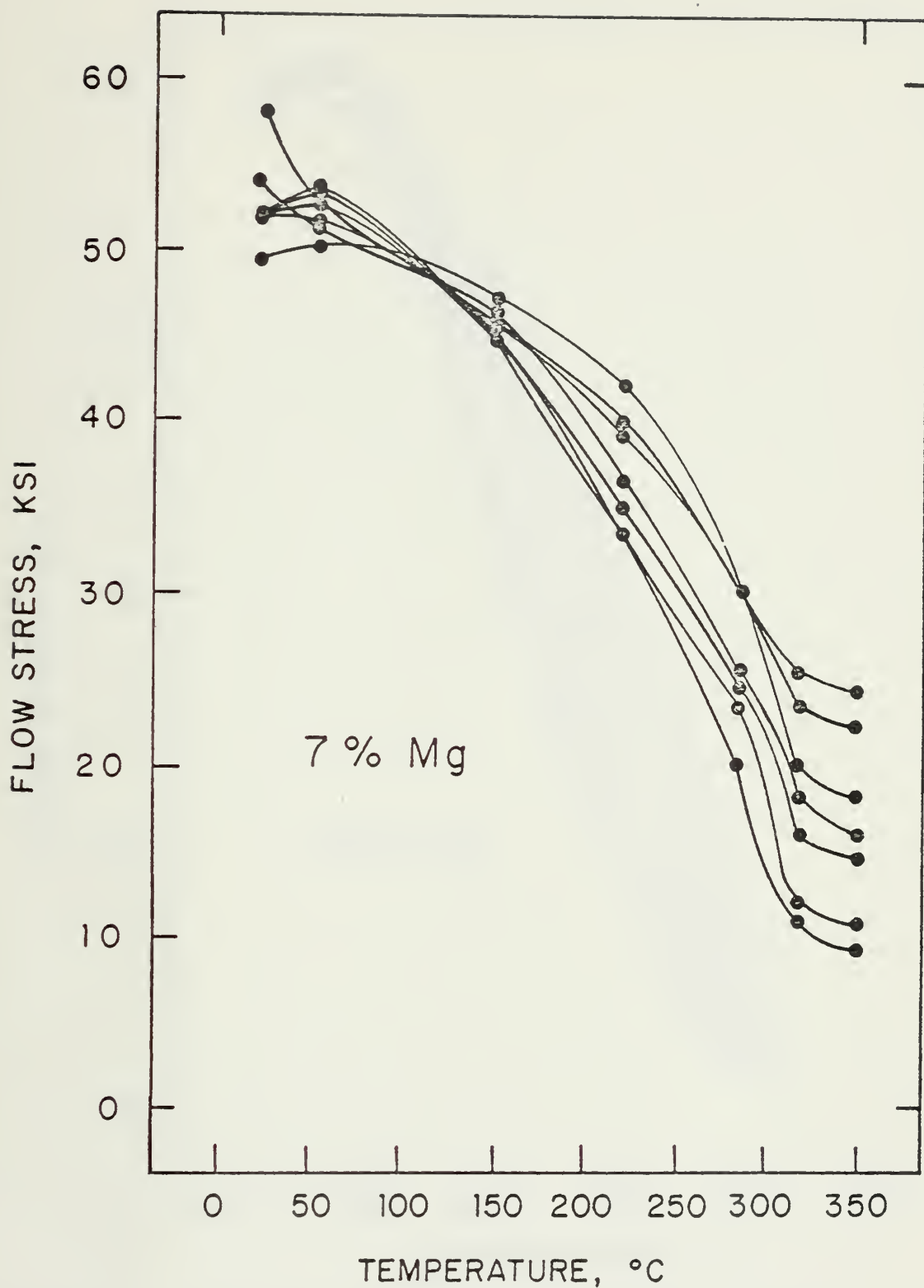


Figure 22. Flow stress vs. temperature for 7% Mg alloy at several strain rates. Flow stress varies directly with strain rate and inversely with temperature. The change in slope at 315°C corresponds to crossing solvus for a 7% Mg alloy. The strain rates employed are given in Table I.

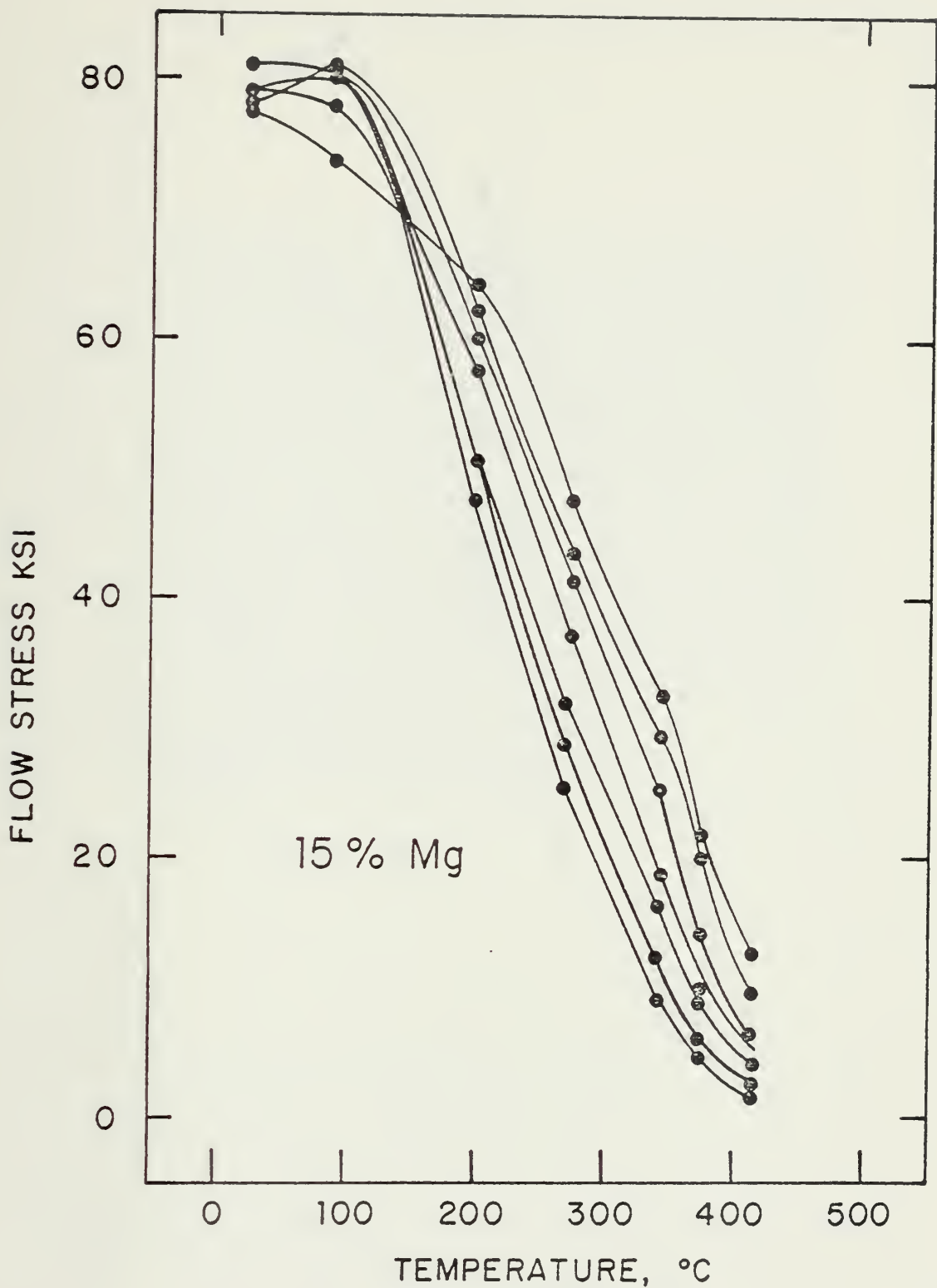


Figure 23. Flow stress vs. temperature for 15% Mg alloy at several strain rates. Flow stress varies directly with strain rate and inversely with temperature. The strain rates are given in Table II.

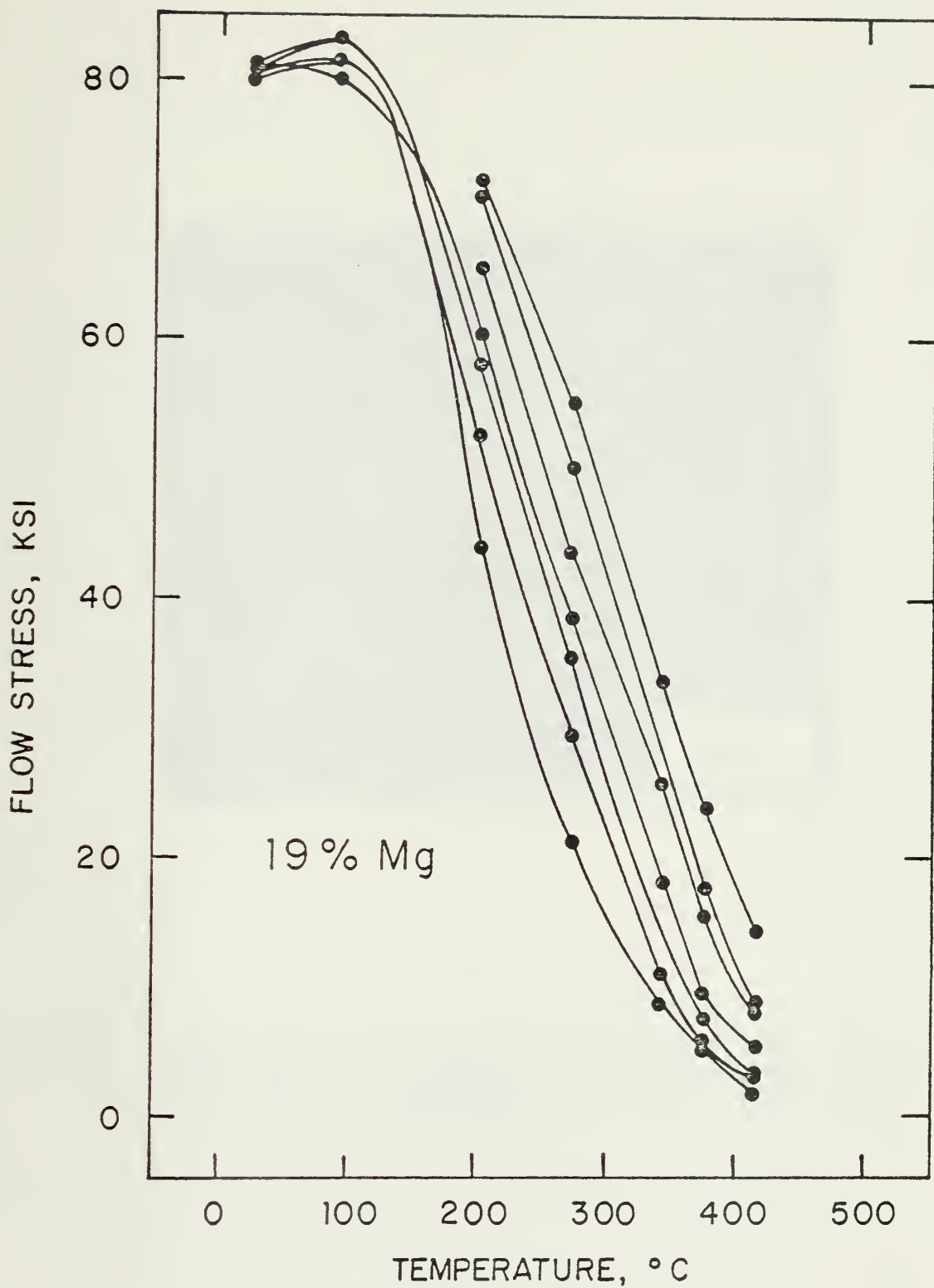


Figure 24. Flow stress vs. temperature for 19% Mg alloy at several strain rates. Strain rates are given in Table II.

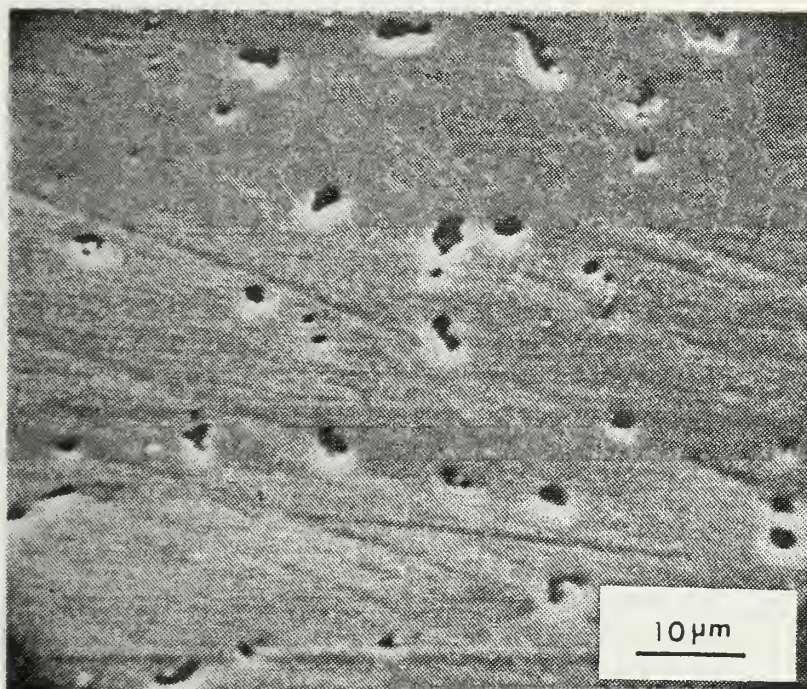


Figure 25. SEM photomicrograph of an as-cast 7% Mg alloy. Small amount of intermetallic beta phase (dark particles) is indicative of alloys containing less than 10% Mg, 1400X.

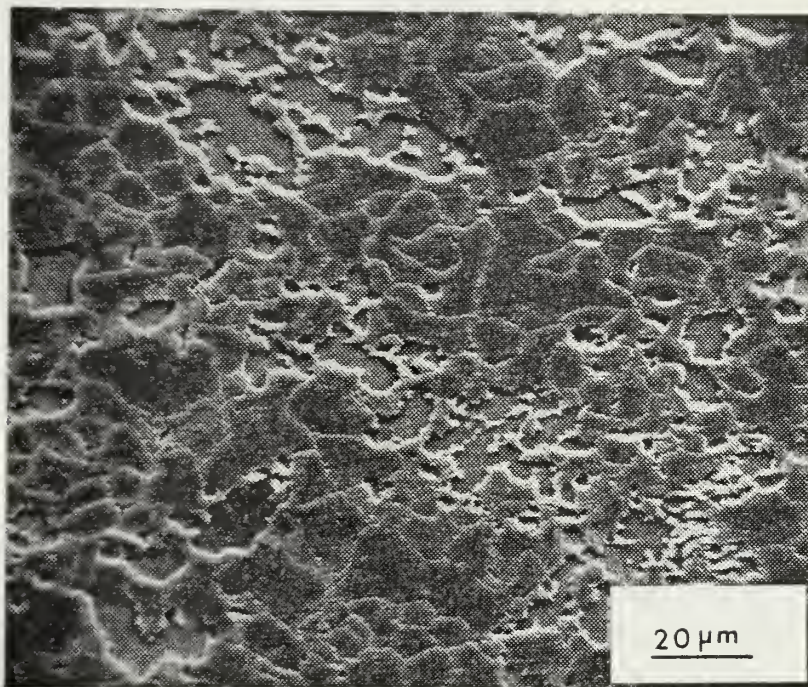
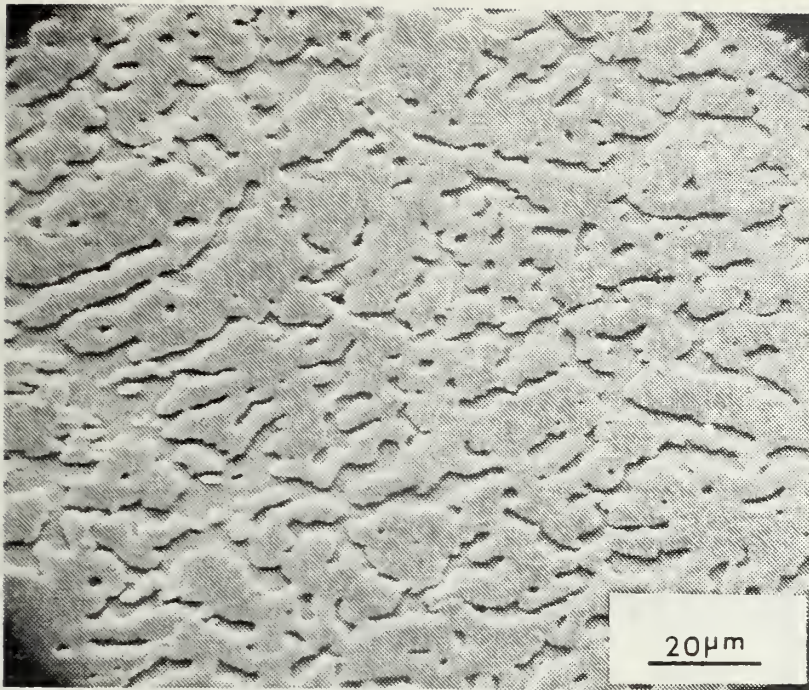
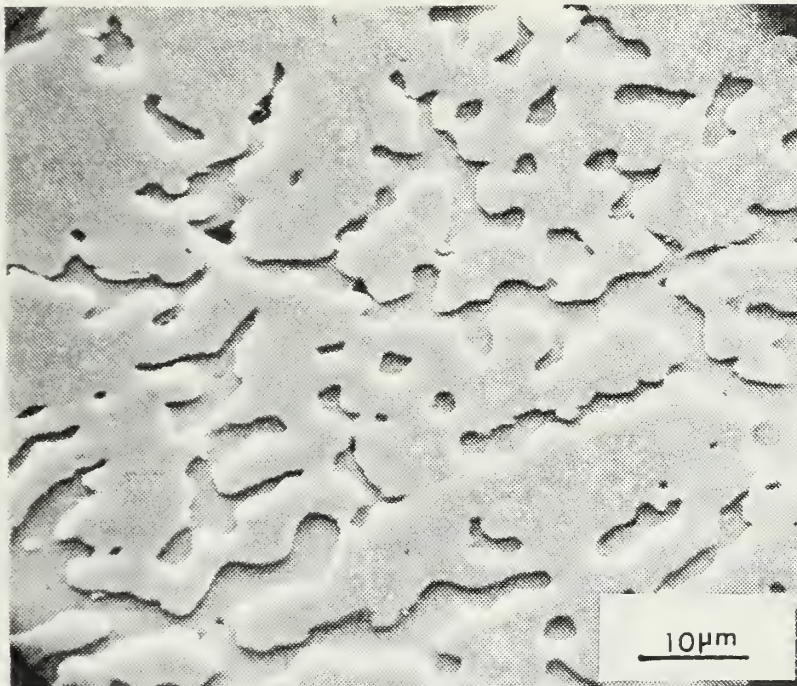


Figure 26. SEM photomicrograph of a 15% Mg specimen following compression testing. Test conditions: $T = 414^{\circ}\text{C}$, $\dot{\epsilon} = 1.3 \times 10^{-3} \text{ sec}^{-1}$, followed by $1.3 \times 10^{-2} \text{ sec}^{-1}$, total strain during compression test = .49. Beta has broken up much more than during upsetting. Also, fine beta appears to be forming in the alpha matrix, mostly along grain boundaries.

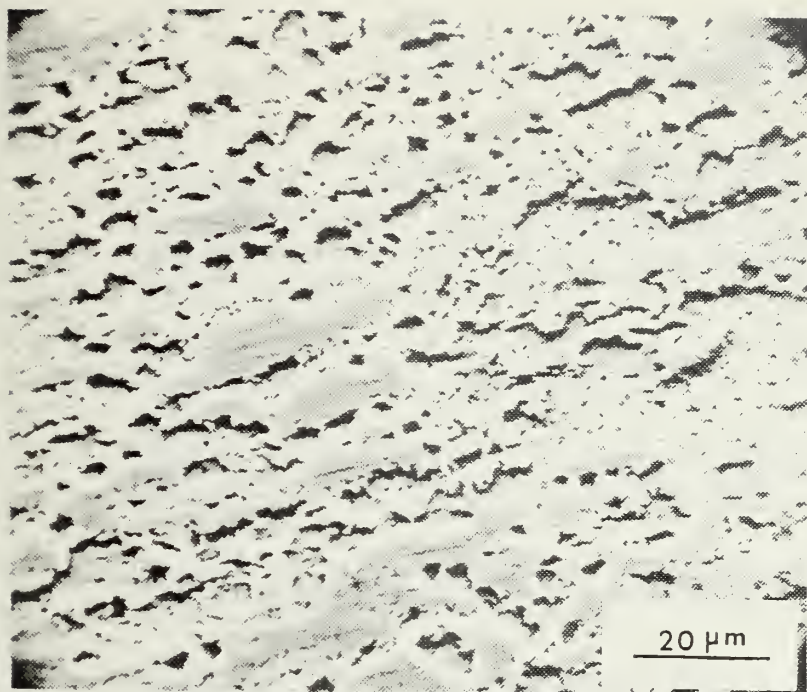


710X

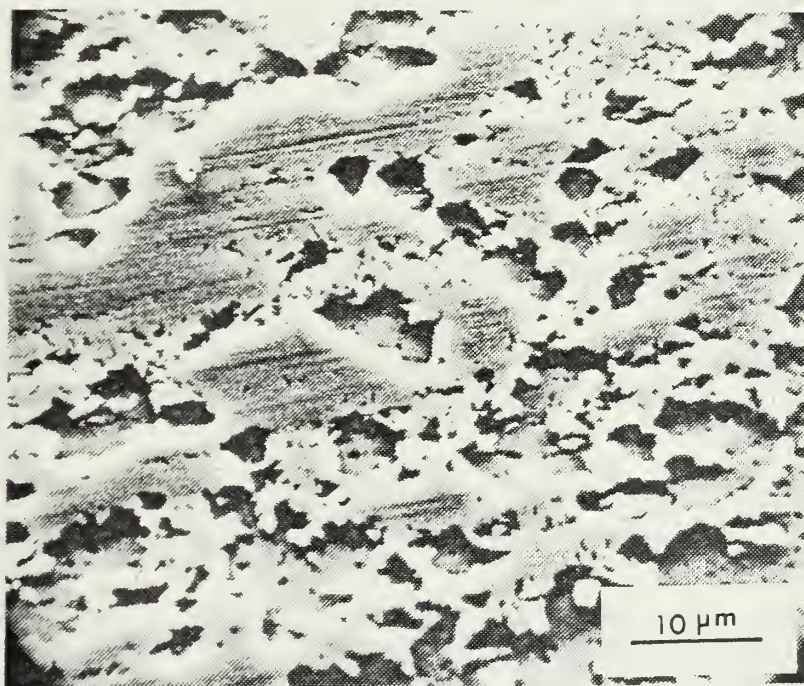


1410X

Figure 27. Recast 19% Mg alloy with addition of 0.3% (by weight) Fe. The beta microstructure is greatly refined and much less continuous than 19% Mg as-cast alloy. This is greatly due to quenching procedures but also due to addition of Fe.



840X



1700X

Figure 28. Recast 19% Mg alloy with addition of 0.3% Fe following upsetting at 300°C. Note the presence of finer and more homogeneous dispersion of beta particles in comparison to Figure 25.

LIST OF REFERENCES

1. Bly, D.L., Sherby, O.D., and Young, C.M., "Influence of Thermal Mechanical Treatments on the Mechanical Properties of a Finely Spheroidized Eutectic - Composition Steel," Materials Science and Engineering, V. 12, p. 41-46, 1973.
2. Sherby, O.D., "Superplasticity," Science Journal, V. 5, No. 6, p. 75-80, June 1969.
3. Alden, T.H., "Review Topics in Superplasticity," Treatise on Materials Science and Technology, V. 6, p. 227-231, 247-249, 1975.
4. Source Book on Materials Selection, V. 2, p. 327-331, American Society for Metals, 1977.
5. Hayde, H.W., W.G. Moffatt, and J. Wueff, The Structure and Properties of Materials, V. 3, p. 84-89, Wiley, 1965.
6. Barrett, C.R., Nix, W.D., and Tetelman, A.S., The Principles of Engineering Materials, p. 202-211, 258-275, Prentice-Hall, 1973.
7. Dieter, G.E., Mechanical Metallurgy, 2nd ed., p. 190-193, 208-210, 340-353, 550-552, McGraw-Hill, 1976.
8. Brick, R.M., Pense, A.W., and Gordon, R.B., Structure and Properties of Engineering Materials, 4th ed., p. 109-113, 251-252, McGraw-Hill, 1977.
9. Ashby, M.F. and Verrall, R.A., "Diffusion-Accommodated Flow and Superplasticity," ACTA Metallurgica, V. 21, p. 149-163, February 1973.
10. Savitsky, E.M., The Influence of Temperature on the Mechanical Properties of Metals and Alloys, p. 238-252, Oxford University Press, 1962.
11. Ness, F.G., High Strength to Weight Aluminum - 18 Weight Percent Magnesium Alloy Through Thermal Mechanical Processing, Masters Thesis, Naval Postgraduate School, 1976.
12. Bingay, C.P., Microstructural Response of Al-Mg Alloys to Thermomechanical Processing, Masters Thesis, Naval Postgraduate School, 1977.

13. Sherby, O.D. and Burke, P.M., "Mechanical Behavior of Crystalline Solids at Elevated Temperature," Progress in Materials Science, V. 13, p. 325-386, 1968.
14. Ayers, R.A., "Enhanced Ductility in an Aluminum-4 PCT Magnesium Alloy at Elevated Temperature," Metallurgical Transactions, V. 8A, No. 3, p. 487-492, March 1977.
15. Sperry, P.R. and Bankard, M.H., "Metallographic Technique for Aluminum Alloys," Metals Handbook 8th ed. Volume 8, p. 120-129, 1973.
16. Burton, M.S., Applied Metallurgy for Engineers, p. 241-242, McGraw-Hill, 1956.

INITIAL DISTRIBUTION LIST

	No. Copies
1. Defense Documentation Center Cameron Station Alexandria, VA 22314	2
2. Library, Code 0212 Naval Postgraduate School Monterey, CA 93940	2
3. Department Chairman, Code 69 Department of Mechanical Engineering Naval Postgraduate School Monterey, CA 93940	2
4. Professor T.R. McNelley, Code 69Mc Department of Mechanical Engineering Naval Postgraduate School Monterey, CA 93940	5
5. Professor A.J. Perkins, Code 69Ps Department of Mechanical Engineering Naval Postgraduate School Monterey, CA 93940	1
6. LT Terry L. Glover 5524 N. Grandview Little Rock, AR 72207	2

4 APR 78
23 AUG 79

S11822
25306

172792

Thesis
G5085
c.1

Glover
Effects of thermo-
mechanical processing
on aluminum-magnesium
alloys containing high
weight percentage mag-
nesium.

4 APR 78
23 AUG 79
23 AUG 79

S11822
25306
25306

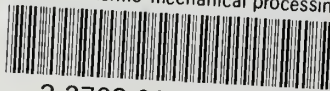
Thesis
G5085
c.1

Glover
Effects of thermo-
mechanical processing
on aluminum-magnesium
alloys containing high
weight percentage mag-
nesium.

172792

thesG5085

Effects of thermo-mechanical processing



3 2768 002 02950 6

DUDLEY KNOX LIBRARY 0.1